

CHAPTER-VI

HEAT BUDGET OF THE OCEANS

The main source of energy for the earth and its environment is the sun. At the outer limit of the earth's atmosphere the intensity of solar energy incident on a surface at right angles to the solar beam is nearly equal to $2 \text{ gm.cal.cm}^{-2} \text{ min}^{-1}$ (langley's per day), which is called solar constant. The earth intercepts a circular sample of this radiation which has an area of πR^2 . The earth's daily rotation distributes this sample of energy over the spherical surface of the earth, which has an area of $4\pi R^2$. As a result the average input of solar radiation at the top of the atmosphere is $\pi R^2/4\pi R^2 = 0.5 \text{ gm.cal.cm}^{-2} \text{ min}^{-1}$ (ly/day).

Our experience over few decades established that the average temperature of the oceans is maintained constant which amounts that the gains and losses of heat by the oceans are balanced with each other. This balance of losses and gains of heat is called the heat budget.

Heat per unit volume is computed from temperature using $Q = (\text{density} \times \text{specific heat} \times T)$ where Q is heat/volume and T is temperature in degrees Kelvin. (When making a heat calculation within the ocean, where pressure is non-zero, uses potential temperature. MKS units of heat are joules. Heat change is expressed in Watts (i.e. joules/sec). Heat flux is in Watts/meter² (energy per second per unit area).

To change the temperature by 1°C in a column of water of 100 m thick and a surface area of 1 m^2 on the top to bottom, over a period of 30 days, requires what heat flux? The density of sea water is about 1025 kg/m^3 and the specific heat is about 3850 J/(kg C) . The heat flux into the volume must then be $\frac{\rho C_p \Delta T V}{\Delta t}$ where T is temperature and t is time. This gives a heat change of 100 W. The heat flux through the surface area of 1 m^2 is thus 100 W/m^2 .

However, the practical calculation of the heat content H (Jm^{-2}) in the water column is:

$$H = \rho_w C_{pw} \int_0^z T dz, \text{ where } \rho_w \text{ is the density of sea water (1000 kg m}^{-3}\text{) and } C_{pw} \text{ is the specific}$$

heat capacity of water ($3.94 \text{ Joules g}^{-1} \text{ }^\circ\text{C}^{-1}$) at constant pressure and Z is the vertical coordinate with positive downward.

Oceans play an important role in the global climate system. They absorb most of the incoming shortwave radiation entering the earth's atmosphere and redistribute heat energy within the oceanic environment by both horizontal and vertical movements. This energy is then further transported back into the atmosphere in the form of latent and sensible heat fluxes and long wave radiation, which are the main sources of energy for the atmospheric circulation. Latent heat flux results from evaporation at the ocean surface. As water changes from liquid to vapor, the ocean loses energy in the form of latent heat of vaporization and the atmosphere gains heat when the vapor condenses. Since water vapor pressure depends on temperature, SST is an important parameter in determining the latent heat flux. The sensible heat flux is a function of the temperature difference between the ocean surface and the atmosphere immediately above. Both the latent heat flux and the sensible heat flux are controlled by the characteristics of atmospheric boundary layer (water vapor content, wind speed and atmospheric stability). The net heat flux at

the ocean surface is the balance between incoming short and long wave radiations, the heat loss by outgoing long wave radiation, evaporation (latent heat), and to some extent by the surface turbulent fluxes of sensible heat.

Despite the positive radiation balance at low latitudes, and the negative balance at high latitudes, there is no evidence that low latitudes are warming and high latitudes are cooling steadily. Therefore there must be transport of heat from low to high latitudes through the atmospheric wind systems as well as the ocean currents. Thus between the low to high latitudes a big thermodynamic engine is working with a source in the low latitudes and a sink in the high latitudes. This is what is known as the general circulation of ocean and atmosphere.

GAINS:

- Direct radiation from the sun (Insolation), $Q_S = 320 \text{ ly/day}$
- Heat flow through ocean floor (0.1 ly/day)
- Conversion of kinetic energy of waves into heat in the surf zone of coastal oceans
- Heating through bio-chemical processes and nuclear reactions inside the oceans
- Advective transfer of heat (rate of heat inflow due to currents), Q_V
- All the gains from 2 to 4 are negligibly small and so are neglected.

LOSSES:

- Heat exchange between the oceans and atmosphere through
- Back radiation, $Q_B = 130 \text{ ly/day}$
- Sensible heat transfer (conduction), $Q_H = 20 \text{ ly/day}$
- Latent heat transfer (evaporation), $Q_E = 170 \text{ ly/day}$

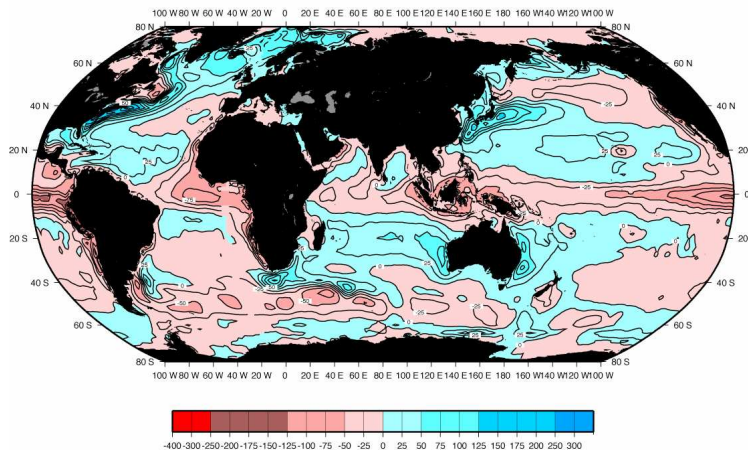


Fig. 6.1. Ocean's heat (W m^{-2}) gain (Red shading) and loss (Blue) (By courtesy of www.nodc.noaa.gov)

Please see Fig.6.1 for the areas of heat gain (red shading) and heat loss (blue shading) in different oceans.

Keeping all these above in mind, we can write the equation for the heat budget for any particular locality as $(Q_S + Q_V) - (Q_B + Q_H + Q_E) = Q_T$ Where Q_T (balance) is the resultant

rate of gain or loss of heat of a body of water at that locality. In low and middle latitudes Q_T is considered as the net heat flux which is shown in fig. 6.2.

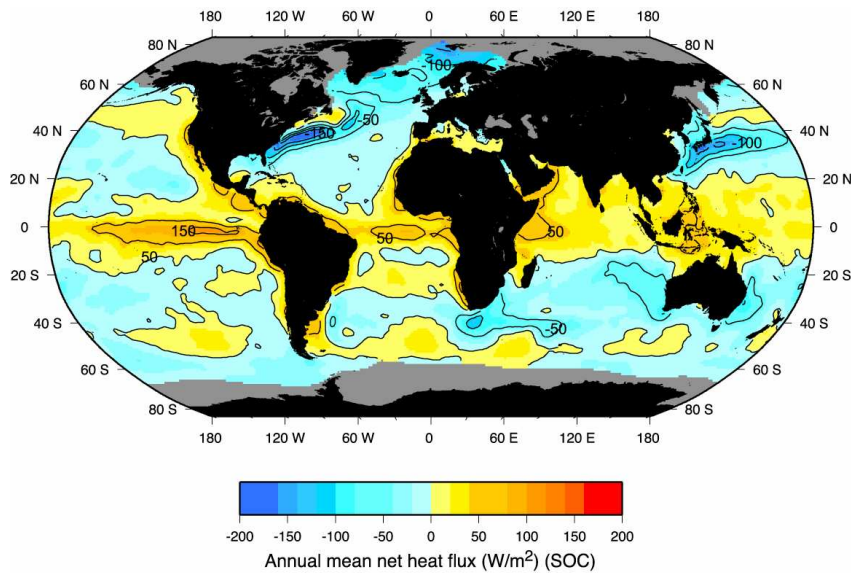


Fig.6.2. Annual mean net heat flux (W/m^2) over the oceans (By courtesy of www.nodc.noaa.gov)

If $Q_T = 0$ means the temperature of the body of water is not changing. This does not mean that there is no heat exchange. It simply means that the net inflow equals the net out flow which is a steady state condition.

If we apply this to the world oceans as a whole, $Q_V = 0$ because all the advective flows are internal and must add up to zero as the average temperature of the world oceans remains constant.

If we average over a whole year or a number of years the seasonal changes average out and Q_T becomes zero.

Then the heat budget equation can be written as $(Q_S + Q_V) - (Q_B + Q_H + Q_E) = 0$

or $Q_S = Q_B + Q_H + Q_E$ Mosby has calculated the average values as

$320 = 130 + 20 + 170$ (which means 38% + 6% + 56% of Q_S). These values give some idea of the average magnitude of the heat budget terms. Fig.6.3 shows the different legs showing the heat gains and losses of the heat budget.

6.1. Net Radiation and the Planetary Energy Balance:

Shortwave radiation from the Sun enters the surface-atmosphere system of the Earth and is ultimately returned to space as longwave radiation (because the Earth is cooler than the Sun). A basic necessity of this energy interchange is that incoming solar insolation and outgoing radiation be equal in quantity. One way of modeling this balance in energy exchange is described graphically with the use of the following two cascade diagrams.

The Global Shortwave Radiation Cascade describes the relative amounts (based on 100 units available at the top of the atmosphere) of shortwave radiation partitioned to various atmospheric processes as it passes through the atmosphere. The diagram indicates that 19 units of insolation are absorbed (and therefore transferred into heat energy and) in the atmosphere by the following two processes:

- Stratospheric Absorption of the Ultraviolet Radiation by Ozone 2 units; and
- Tropospheric Absorption of Insolation by Clouds and Aerosols 17 units.

23 units of solar radiation are scattered in the atmosphere subsequently absorbed at the surface as diffused insolation. 28 units of the incoming solar radiation are absorbed at the surface as direct insolation. Thus the total amount of solar insolation absorbed at the surface equals 51 (28+23) units. The total amount of shortwave radiation absorbed at the surface and in the atmosphere is 70 (2+17+28+23) units.

Three main losses of solar radiation back to space through reflection occur in the Earth's shortwave radiation cascade. 4 units of sunlight are returned to space from surface reflection. Cloud reflection returns another 20 units of solar radiation. Back scattering of sunlight returns 6 units to space. The total loss of shortwave radiation from these processes is 30 (4+6+20) units. The term used to describe the combined effect of all of these shortwave reflection losses is called the Earth's albedo.

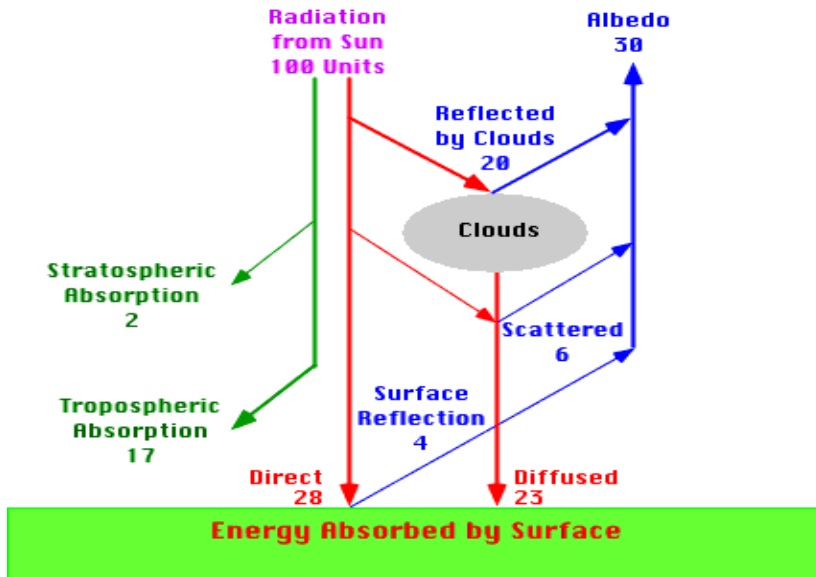


Fig.6. 3 Global Shortwave radiation cascade (www.physicalgeography.net)

The Global Longwave Radiation Cascade indicates that energy leaves the Earth's surface through three different processes. 7 units leave the surface as sensible heat. This heat is transferred into the atmosphere by conduction and convection. The melting and evaporation of water at the Earth and ocean surface incorporates 23 units of energy into the atmosphere as latent heat. This latent heat is released into the atmosphere when the water condenses or becomes solid. Both of these processes become part of the emission of longwave radiation by the atmosphere and clouds.

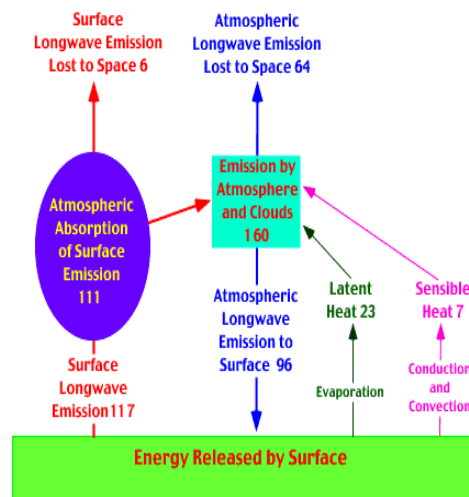


Fig.6. 4 Global long wave radiation cascade (www.physicalgeography.net)

The surface of the Earth and ocean emits 117 units of longwave radiation. Of this emission only 6 units are directly lost to space. The other 111 units are absorbed by

greenhouse gases of the atmosphere and converted into heat energy and then into atmospheric emissions of longwave radiation (the greenhouse effect).

The atmosphere emits 160 units of longwave energy. Contributions to this 160 units are from surface emissions of longwave radiation (111 units), latent heat transfer (23 units), sensible heat transfer (7 units), and the absorption of shortwave radiation by atmospheric gases and clouds (19 units, see Figure 6.4) . Atmospheric emissions travel in two directions. 64 units of atmospheric emissions are lost directly to space. 96 units travel to the Earth's surface where it is absorbed and transferred into heat energy.

The total amount of energy lost to space in the global longwave radiation cascade is 70 units (surface emission 6 units + atmospheric emission 64 units). Please note that this is the same amount of energy (2+17+28+23=70 units) that was added to the Earth's atmosphere and surface by the Global Shortwave Radiation Cascade.

Finally, to balance the surface energy exchanges in this cascade we have to account for 51 units of missing energy [atmosphere and cloud longwave emission (96 units) minus surface longwave emission (117 units) minus latent heat transfer (23 units) minus sensible heat transfer (7 units) = -51 units].

$$96-117-23-7 = -51$$

This missing component to the radiation balance is the 51 units of energy absorbed at the Earth's surface as direct and diffused shortwave radiation (Figure 6.4).

The following equations can be used to mathematically model the shortwave radiation balance, longwave radiation balance and the net radiation balance for the Earth's surface at a single location or for the whole globe for any temporal period:

$$K^* = (K + k)(1 - a)$$

$$L^* = (LD - LU)$$

$$Q^* = (K + k)(1 - a) - LU + LD$$

where

Q* is surface net radiation (global annual values of **Q* = 0** , because input equals output, local values can be positive or negative),

K* is surface **net shortwave radiation**,

K is surface **direct shortwave radiation**,

k is **diffused shortwave radiation (scattered insolation)** at the surface,

a is the **albedo** of surface,

L* is **net longwave radiation** at the surface,

LD is atmospheric **counter-radiation** directed to the Earth's surface, and

LU is **longwave radiation** lost from the Earth's surface.

NASA's Surface Radiation Budget Project has used satellite data, computer models, and meteorological data to determine surface net shortwave radiation, net longwave radiation, and net radiation balances for the period July 1983 to June 1991.

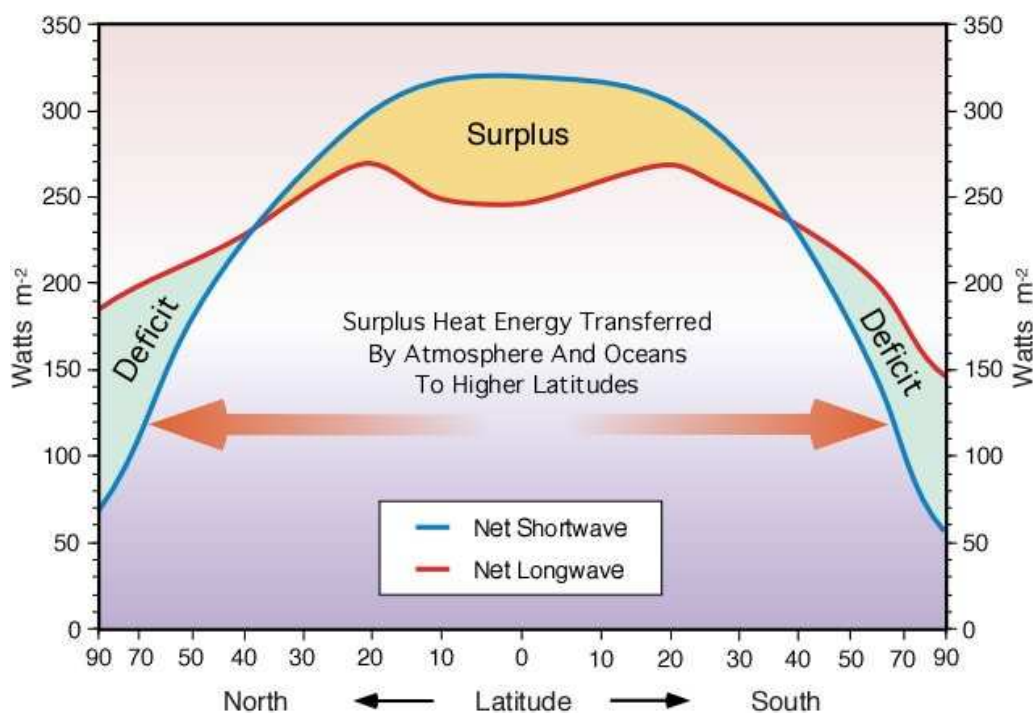


Fig. 6. 5 Balance between average net shortwave and longwave radiation from 90° North to 90° South
(www.physicalgeography.net)

Figure 6.5 illustrates the annual values of net shortwave and net longwave radiation from the South Pole to the North Pole. On closer examination of this graph one notes that the lines representing incoming and outgoing radiation do not have the same

values. From 0 - 35 ° latitude North and South incoming solar radiation exceeds outgoing terrestrial radiation and a surplus of energy exists. The reverse holds true from 35 - 90° latitude north and south and these regions have a deficit of energy. Surplus energy at low latitudes and a deficit at high latitudes results in energy transfer from the equator to the poles. It is this meridional transport of energy that causes atmospheric and oceanic circulation. If there were no energy transfer, the poles would be 25° Celsius cooler, and the equator 14° Celsius warmer!

The redistribution of energy across the Earth's surface is accomplished primarily through three processes: sensible heat flux, latent heat flux, and surface heat flux into oceans. Sensible heat flux is the process where heat energy is transferred from the Earth's surface to the atmosphere by conduction and convection. This energy is then moved from the tropics to the poles by advection, creating atmospheric circulation. As a result, atmospheric circulation moves warm tropical air to the Polar Regions and cold air from the poles to the equator. Latent heat flux moves energy globally when solid and liquid water is converted into vapor. This vapor is often moved by atmospheric circulation vertically and horizontally to cooler locations where it is condensed as rain or is deposited as snow releasing the heat energy stored within it. Finally, large quantities of radiation energy are transferred into the Earth's tropical oceans. The energy enters these water bodies at the surface when absorbed radiation is converted into heat energy. The warmed surface water is then transferred downward into the water column by conduction and convection. Horizontal transfer of this heat energy from the equator to the poles is accomplished by ocean currents.

The following equation describes the partitioning of heat energy at the Earth's surface:

$$Q^* = H \text{ (Sensible heat)} + L \text{ (Latent heat)} + S \text{ (Surface heat flux into soil or water)}$$

- Presence or absence of water in liquid and solid forms at the surface.
- Specific heat of the surface receiving the net radiation.
- Convective and conductive characteristics of the receiving surface.
- Diffusion characteristics of the surface's overlying atmosphere.

6.2. INSOLATION (Incoming solar radiation) (Q_s):

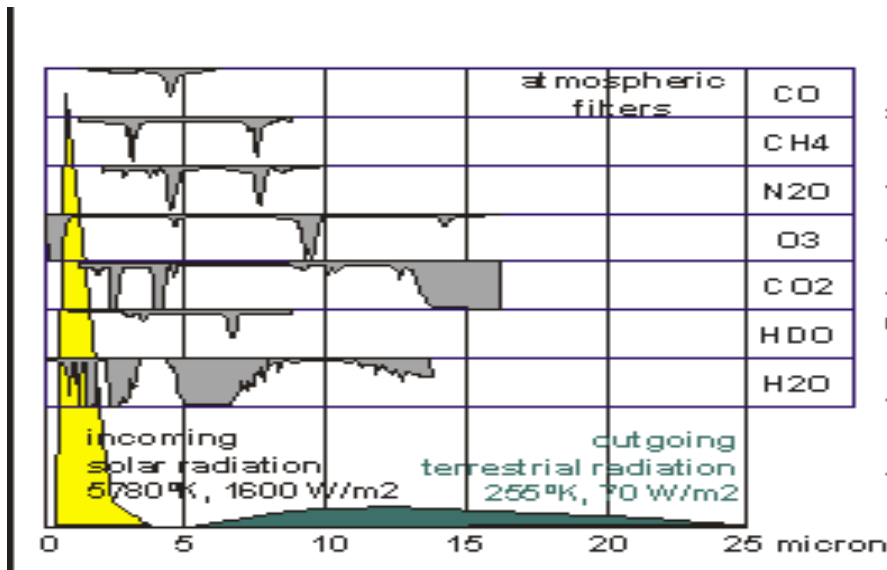


Fig.6.6a. Solar and terrestrial radiation

The fig. 6.6a shows the solar and terrestrial radiation curves. The yellow curve is the solar radiation reaching the earth's upper atmosphere. The green curve is the terrestrial radiation leaving the earth's surface. In between them is the atmosphere with its various gases that filter the radiation both ways (grey curves). In addition sunlight is reflected by the surface of the earth and the clouds. Horizontal x-axis is wave length in micro-meters and the vertical scale is linear.

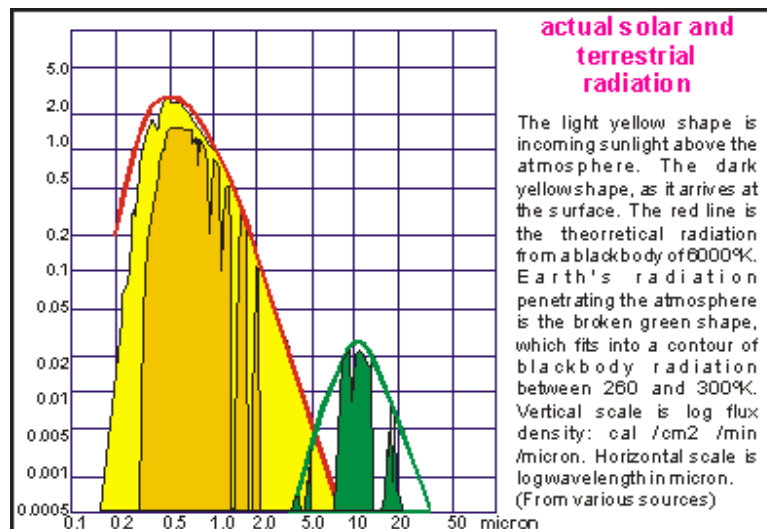


Fig.6.6b. Actual measured solar and terrestrial radiation.

Fig.6.6b. shows the actual measured solar and terrestrial radiation. The light yellow area is the incoming sunlight above the atmosphere. The dark yellow area is as it arrives at the surface. The red curve is the theoretical Stefan-Boltzman radiation from a black body of 6000°K. Earth's radiation penetrating the atmosphere is the broken green curve which fits into a contour of black

body radiation between 260 and 300^oK. Horizontal scale is long wave length in micron and the vertical scale is log flux density in cal/cm²/min/micron.

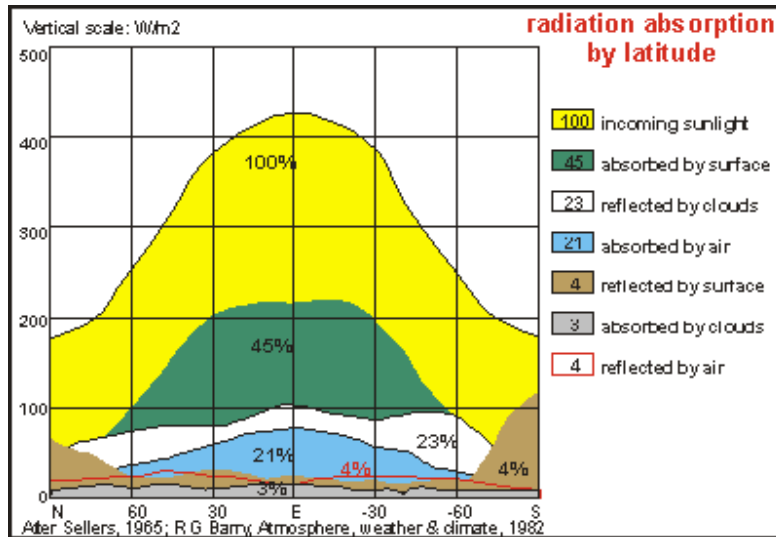


Fig.6.6c Absorption of radiation at different latitudes.

The fate of radiation entering the earth and its environment is shown in Fig.6.6c. Out of 100% incoming radiation, 45% is absorbed by the earth's surface, 23% is reflected by clouds, 21% is absorbed by various gases in the atmosphere, 4% reflected by the earth's surface, 3% is absorbed by the clouds and 4% reflected by air molecules.

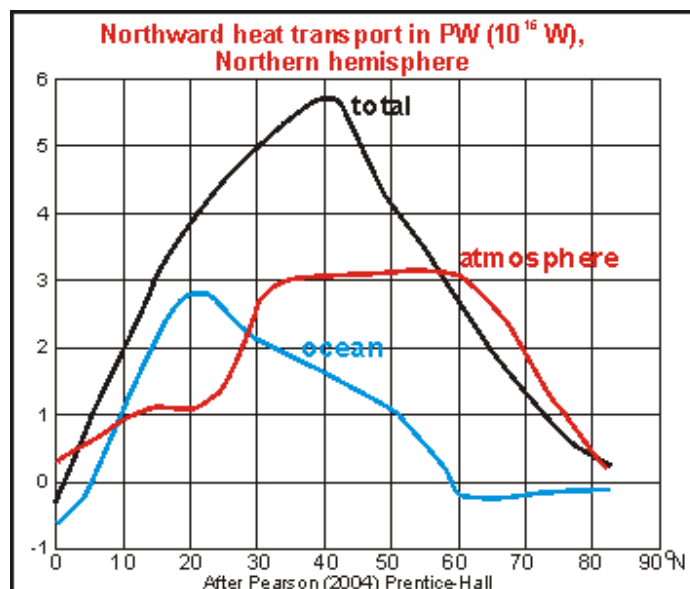


Fig.6.6d. Northward transport of heat in Northern Hemisphere in peta watts.

Fig.(6.6d) shows Northward transport of heat in Northern Hemisphere in peta watts in different latitudes through the oceans and atmosphere. While the total radiation is transported

maximum at 40°N , through oceans it is at 20°N and through the atmosphere it is between 35° - 60°N . The heat transport through atmosphere is higher than the oceans.

As the Earth rotates around its axis, day and night occur. Its, once a year, revolution around the sun (Fig.6.6e) would have been unnoticeable if the Earth's axis of rotation had not been tilted. Its tilt of 23.5° creates the seasons, which means, that every place on the earth experiences at least once a year, a period of intense sunlight, bright enough for life to blossom. As the path of the earth around the sun is elliptical, it stands closest (perihelion) to the sun in the June solstice, the northern summer and the farthest (aphelion) in December solstice. Being 1.7% closer, lands 3.4% more sunlight on the outer atmosphere, which is a noticeable amount in the radiation balance. But it is not only this that makes the northern summers warmer.

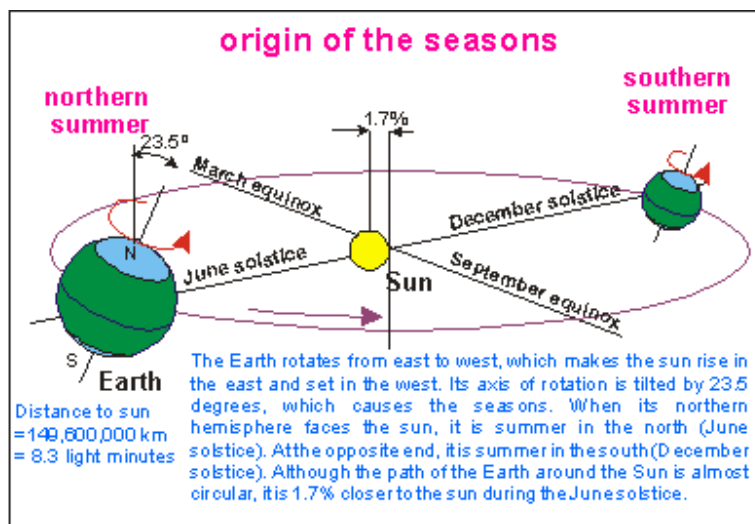


Fig.6.6e. Formation of seasons due to revolution and inclination of the earth's axis

Figure (6.6f) below describes the potential insolation available for the equator and several locations in the Northern Hemisphere over a one-year period. The values plotted on this graph take into account the combined effects of angle of incidence and day length duration. Locations at the equator show the least amount of variation in insolation over a one-year period. These slight changes in insolation result only from the annual changes in the altitude of the Sun above the horizon, as the duration of daylight at the equator is always 12 hours. The peaks in insolation intensity correspond to the two equinoxes when the Sun is directly overhead. The two annual minima of insolation occur on the solstices when the maximum height of the Sun above the horizon reaches an angle of 66.5° .

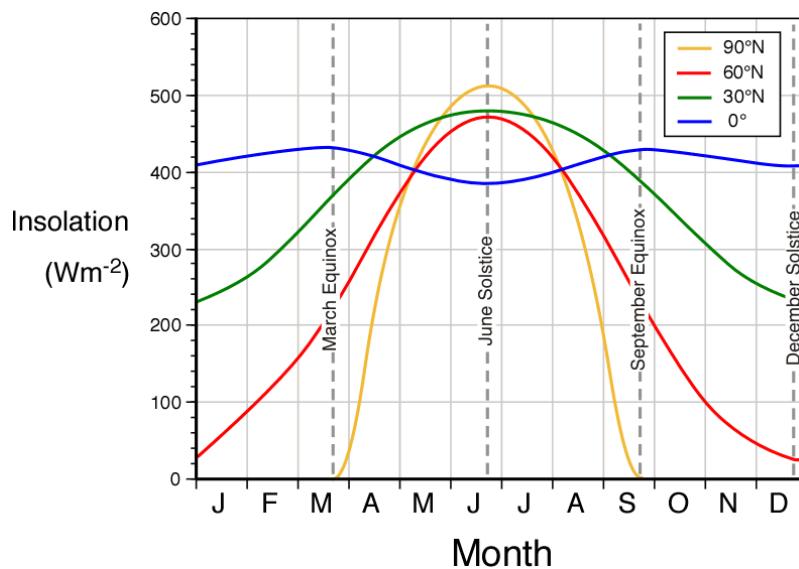


Fig.6.6f. Annual variations in day length for locations at the equator, 30, 50, 60, and 70° North latitude (www.physicalgeography.net)

The most extreme variations in insolation received in the Northern Hemisphere occur at 90°N. During the June (summer solstice), any location in northern hemisphere receives more potential incoming solar radiation than any other location in southern hemisphere. At this time the Sun never sets. In fact, it remains at an altitude of 23.5 degrees above the horizon for the whole day. From September 22 (Autumnal equinox) to March 21, (Vernal equinox) no insolation is received at 90°N. During this period the Sun slips below the horizon as the northern axis of the Earth has an orientation that is tilted away from the Sun

The annual insolation curve for locations at 60 degrees North best approximates the seasonal changes in solar radiation intensity perceived at our latitude. Maximum values of insolation are received at the June (summer solstice) when day length and angle of incidence are at their maximum. During the June (summer solstice) day length is 18 hours and 27 minutes and the angle of the Sun reaches a maximum value of 53.5 degrees above the horizon. Minimum values of insolation are received during the December (winter solstice) when day length and angle of incidence are at their minimum. During the December solstice day length is only 5 hours and 33 minutes and the angle of the Sun reaches a lowest value of 6.5 degrees above the horizon.

As the Fig (6.6g) shows, the tilt of the Earth has a profound effect on the amount of sunshine falling on its surface. In the tropics, seasonal variation is hardly noticeable (14%, twice yearly) but in temperate climates like New Zealand, the summer brings three times more sunlight (arising from both duration and intensity), than winter. For the poles, the difference is of course extreme, due to the polar night. Ironically, the amount of sunlight experienced in the polar summer, exceeds that in the tropics, due to the 24 hour polar summer day. For sea life, these curves are very important.

Also on a daily basis, as we all know, the sunlight changes strength as we pass from night to day and into night again. The curve on the right shows the theoretical decline of sunlight intensity, depending on the sun's angle from vertical. Notice how steeply it drops off towards sunset/sunrise. By 7:30 AM and 4:30 PM (assuming 12 hours daylight), the sun has reached half strength. For example if a place like New Zealand is located roughly at 40°S, the sun's angle

varies from $40 + 23.5 = 63.5^\circ$ in summer to $40 - 23.5 = 16.5^\circ$ in winter, measured from direct overhead. This corresponds to about 40% variation in light intensity.

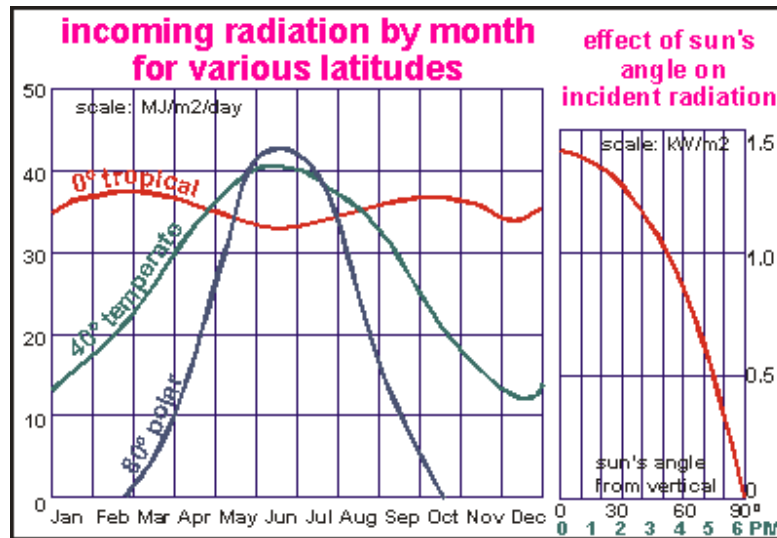


Fig.6.6g. Monthly variation of insolation in different latitudinal zones

One may note in this regard there is a lag of heat on the earth's surface i.e it takes some time by the earth's surface to get heated even after winter solstice is completed. The reasons are:

- The earth's surface temperature is in a sensitive balance between incoming and outgoing radiation. After the winter solstice, the incoming radiation is undeniably increasing.
- The temperature at any one place on earth does not only depend on the above, but also on the temperature of surrounding land and sea.
- Ice formation is a slow and energy-absorbing process that slows down cooling. Likewise, melting is slow and hinders the warming up. So, once ice has formed, or the temperature passes 0°C , the surface temperature lags considerably.
- Ice and snow bounce back the sunlight, so that the increased solar radiation does not result in more warming.
- Compared to earth and air, water is slow to warm or to cool. Water masses moderate temperature fluctuations.
- Warm water lies on the surface of lakes and seas. Heat is slow to penetrate to deeper layers, but cold water sinks easily to deeper waters. So bodies of water absorb less energy when warming up, but absorb more cold when cooling off (release heat easily).
- Once a body of water starts to freeze over, it absorbs cold more slowly, so its moderating effect becomes much less.
- Water takes a long time and energy to evaporate. So, summer won't begin until (almost) all the winter's rain water has evaporated.

In the absence of atmosphere the incoming solar radiation was computed by Milankovitch with the help of the equation:

$$Q = \int F dt = \frac{24}{\pi} \frac{r_m^2}{r^2} S \sin \phi \sin \delta (H - \tan H)$$

Such that $F = S \cos \theta$, and θ = zenith angle of the sun, r_m = mean distance between sun and earth, r = distance between sun and earth, S = solar constant, ϕ = latitude, δ = declination of the sun, H = hour angle between sun rise and noon.

The Fig.6.7 (Milankovitch diagram) was computed by means of the above equation and shows the dependence of the daily flux of insolation in ly/day on latitude and season in the absence of atmosphere. The horizontal coordinate is given as time of the year in the lower margin and solar declination in the upper margin and the vertical coordinate is the latitude. It is noteworthy that, owing to the length of the day at the summer solstice of the N.H, the North Pole receives the maximum daily total insolation, and the equator receives a minimum. At the winter solstice, these conditions are reversed; indeed latitudes above 68° receive no radiation at all. The total radiation received by the S.H during the southern summer is larger than the amount received by the N.H during its summer, for in the S.H the earth is closer to the sun.

As the direct solar beam shifts seasonally from one hemisphere to the other, the zone of maximum possible daily insolation moves with it. In tropical latitudes the amount of possible insolation is constantly great, and there is little variation with the seasons. But in its annual journey the sun passes over all places between the Tropic of Cancer and the Tropic of Capricorn twice, causing two maxima. Between the latitudes $23\frac{1}{2}$ and $66\frac{1}{2}^\circ$, maximum and minimum periods of insolation occur shortly after the summer and winter solstices, respectively. Beyond the Arctic and Antarctic circles the maximum coincides with the summer solstice, but there is a period during which insolation is lacking. The length of the period is increases toward the poles, where it is of six months duration.

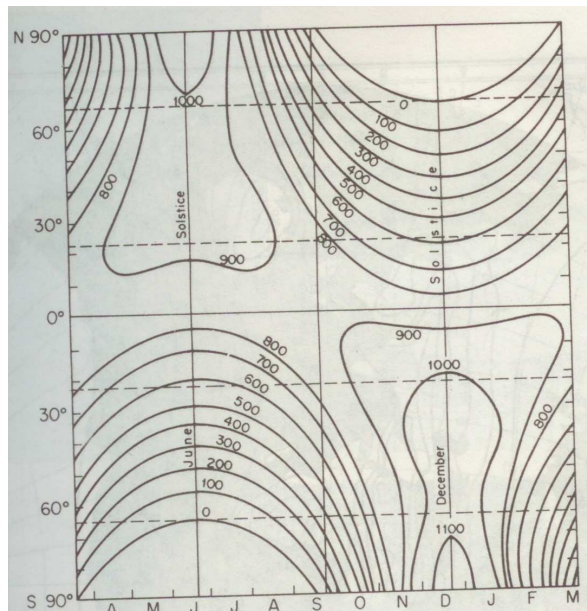


Fig.6. 7. Total daily solar radiation in langley during the year at different latitudes, assuming no atmospheric effects. (After Lamb 1972), based on data calculated by Milankovitch)

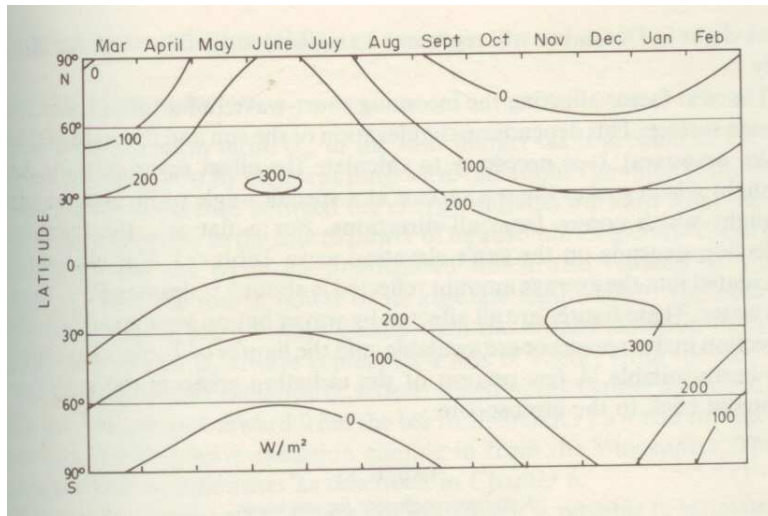


Figure 7.3 Seasonal variation of daily insolation (in 10^6 J m^{-2} at the Earth's surface), assuming 30% reflection from the top of the atmosphere (cf. Section 2.1). Values are highest in mid-latitudes because of long daylengths in summer.

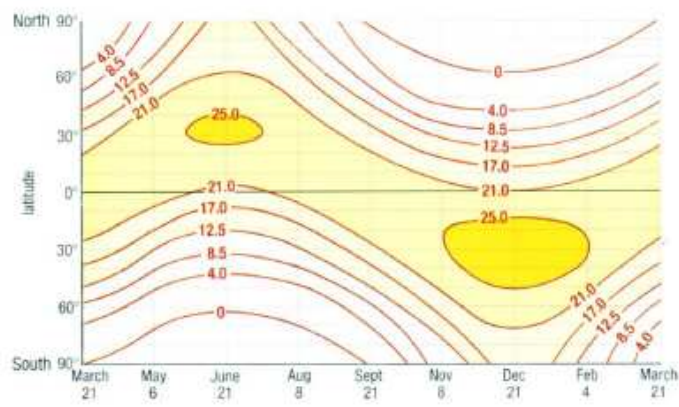


Fig.6. 8 . Daily short wave radiation (Q_s) in watts/m^2 received at the sea surface in the absence of the cloud (Pickard 1985).

Actually the solar radiation received at the earth's surface is somewhat less than that shown in the Fig.6.7 due to the presence of the atmosphere. The depletion of energy in the solar beam is the greatest at high latitudes where because of the large zenith angle; its path through the atmosphere is the longest. For this reason, the region of maximum insolation at the earth's surface is no longer found at the pole in summer but is shifted to about 30° latitude.

The energy penetrating the top of the atmosphere is partly reflected, refracted and scattered. As a consequence of these processes there is a marked change in the intensity of radiant energy that reaches the earth's surface as shown in Fig.6.8. Fig.6.8 shows the daily inflow of Q_s at the earth's surface assuming an average atmospheric transmission of 70% and no clouds as a function of latitude and time of the year. the main features of this diagram are i) the highest values occur at about 30° N and south in the respective summer hemispheres (300 W m^{-2} circle), ii) there is no short wave radiation at poles in the polar winters (0 W m^{-2} lines), iii) the amount of energy input is greater in the southern hemisphere than in the N.H. The reason for this is simply

that the earth is nearer (perihelion position) to the sun during the southern summer than during the northern summer.

Fig.6.8 thus shows that because of the intense reflection of sun light from the snow and ice covered polar caps, the heat energy absorbed by the earth's surface in these regions is small. In a similar way, the cloud bands in the equatorial regions reflect sun light so strongly that the zone of maximum insolation at the earth's surface is shifted into each of the hemispheres to tropics. The inequality of heating of the two hemispheres causes this shift to be asymmetrical as shown in the Fig.6.5.& 6.6. The difference between the ratios of land and sea areas for the two hemispheres is also thought to have something to do with the generally northward shift of the thermal equator.

It can be seen from the comparison of the above two figures (Fig.6.7 & 6.8), the heat absorbed at the earth's surface averages near 0.25 ly/min which means one half of the incident radiation (0.5 ly/min) at the top of the atmosphere. This depletion of energy is caused by direct reflection and scattering of sea surface and clouds of the atmosphere, which is called as albedo of the earth and is approximately equal to 0.34 (34%) over the sea surface.

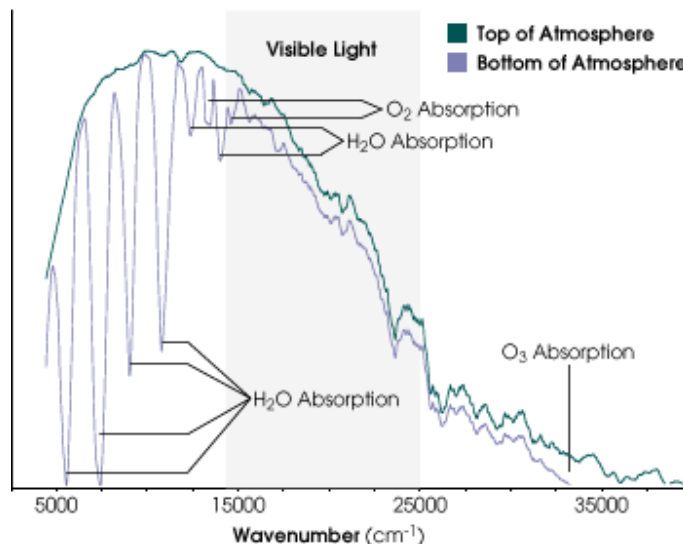


Fig.6.9 . Different stages of absorption of solar radiation (Graph by Robert Simmon, based on model data from the NASA GSFC Laboratory for Atmospheres) . (Courtesy by NASA Langley Research Center).

Fig.6.9 shows the radiation receipt at the surface of the earth after different stages of absorption of solar radiation at sun and atmosphere. Solar radiation is not emitted in a smooth continuum. Superheated atoms in the Sun, particularly Hydrogen and Helium, absorb radiation in distinct wavelengths. These absorption bands are visible as dips in the green line in the graph above, which represents the spectrum of sunlight that arrives at the top of the Earth's atmosphere. Additionally, gas molecules absorb radiation in the Earth's atmosphere, further reducing the radiation at the surface. The blue line represents the spectrum of radiation arriving at the surface of the Earth on a clear day in the tropics, based on an atmospheric model.

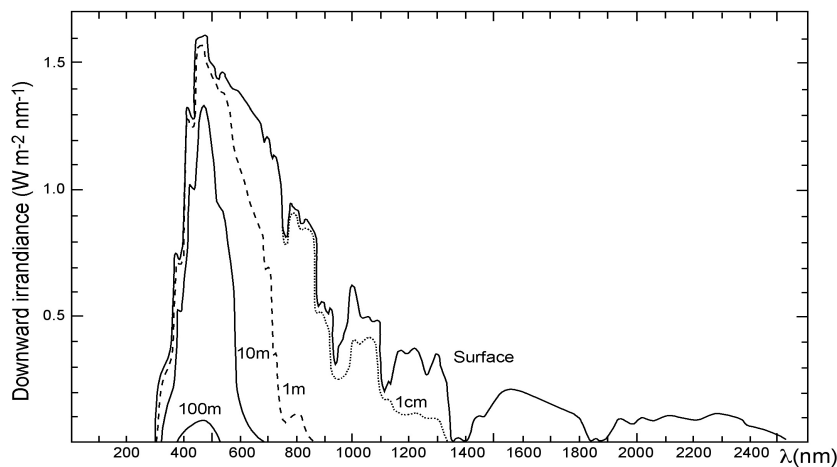


Fig.6. 10 The complete spectrum of insolation (solar irradiance) in the upper 100m of the sea. ($1\text{ nm} = 10^{-9}\text{ m}$, $1\mu = 10^{-6}\text{ m}$, $400\text{ nm} = 0.4\mu$). (Courtesy by NASA Langley Research Center).

Fig.6.10 shows the spectrum of solar radiation that penetrates the sea surface and the subsurface levels. One may note that by the time the solar radiation penetrates to the depth of 100m it lost to $1/50^{\text{th}}$ of the surface value.

6.2.1. DISTRIBUTION OF INSOLATION IN THE OCEANS:

Figs.6.11 & 6.12 shows how SST and the Q_s (W m^{-2}) annually vary over the earth's ocean surface. You can see that the contours appear to be parallel to the latitudes. In the tropical latitudes if you compare the distribution of Q_s between land and ocean over the same latitude it is very interesting. The conspicuous difference is the Q_s is more over the land than the Oceans on the same latitude. The reason for this is the atmosphere over the oceans contains large amount of water vapor which along with different gases like CO_2 , SO_2 etc in the marine atmosphere absorb large amount of solar radiation (about 30%). Whereas the atmosphere over the land is drier and relatively less cloud so there is a chance of penetration of more amount of insolation. However, the effect of water vapor in reducing insolation in low latitudes is greater than that in high latitudes because evaporation occurs at a greater rate from a warmer sea surface than a colder surface. Also as warm air can hold more moisture than the cold air, more water vapor is available in the low latitude atmosphere than the high latitude atmosphere. While the equatorial and tropical oceans receive about $205\text{ J m}^{-2}\text{ yr}^{-1}$ it decreases to less than $80\text{ J m}^{-2}\text{ yr}^{-1}$ in high latitudes in northern hemisphere. In some places (Malaysian and Indonesian region) the effect of water vapor is glaringly seen. While the insolation over the Indonesian region is 150 or so the adjacent East Indian Ocean area is recorded over $200\text{ J m}^{-2}\text{ yr}^{-1}$. The bending of isotherms (Fig.6.9) at coastal places indicates the direction of flow of currents. If the bending is towards low latitudes cold (blue) currents are drifting and if the bending of isotherms are towards higher latitudes (red) warm currents are drifting.

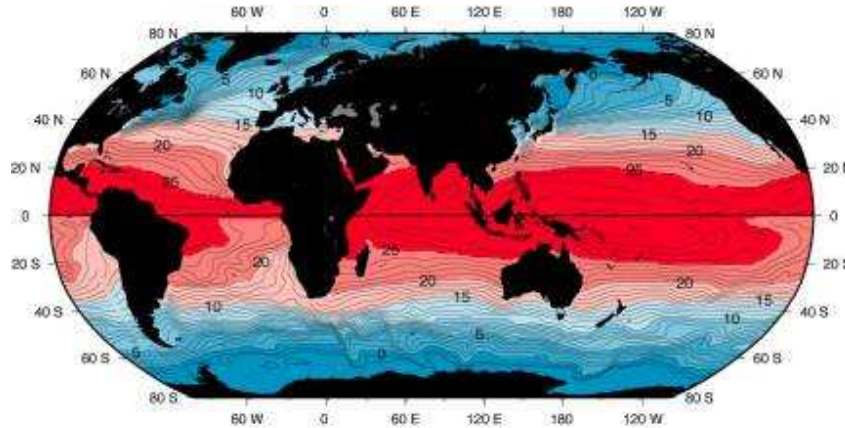


Fig. 6. 11. Global variation of SST (By courtesy of www.nodc.noaa.gov)

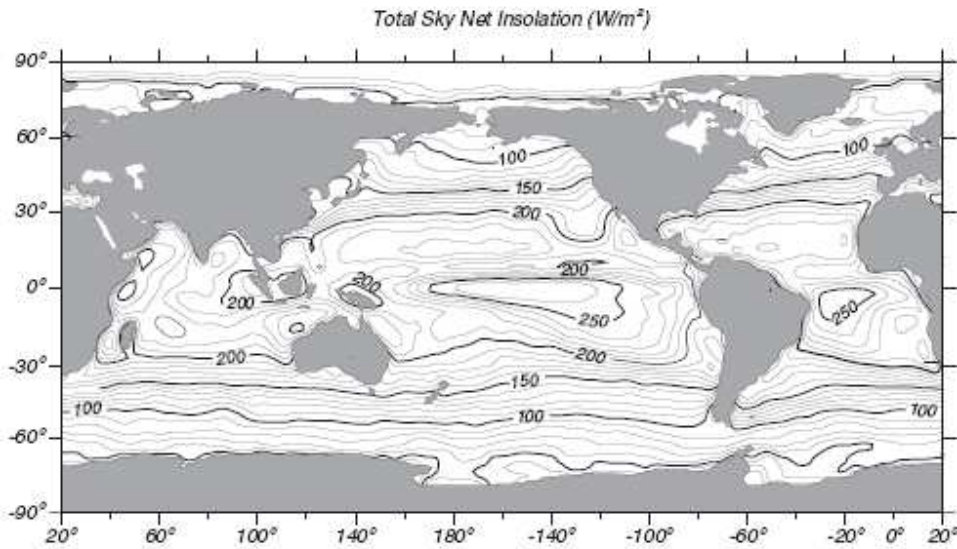


Fig.6.12. Annual mean Q_s in W m^{-2} through the sea surface. (Courtesy by NASA Langley Research Center).

6.2.2. DISTRIBUTION OF INSOLATION IN THE BAY OF BENGAL:

The incoming short wave radiation (SWR) in the Bay of Bengal during January was low and showed a spatial variation of about 25 W/m^2 within the basin, which was lowest compared with other months (Fig.6.13A,a). North of 15°N , SWR showed decreasing trend with a minimum value of 190 W/m^2 very near to the head Bay. In the central Bay SWR varied marginally between 195 and 200 W/m^2 . Highest value of SWR was seen in the Andaman Sea ($\sim 210 \text{ W/m}^2$) and west of Sri Lanka. During June SWR showed a decrease in the northern Bay with highest value of 230 W/m^2 close to the head Bay (Fig.6.13A,b). Along the western boundary SWR was about 220 W/m^2 , which decreased towards the central Bay reaching a minimum value of 195 W/m^2 . From the

central Bay towards the eastern boundary the SWR showed a weak increase. The variation in the SWR from south to north was about 40 W/m^2 .

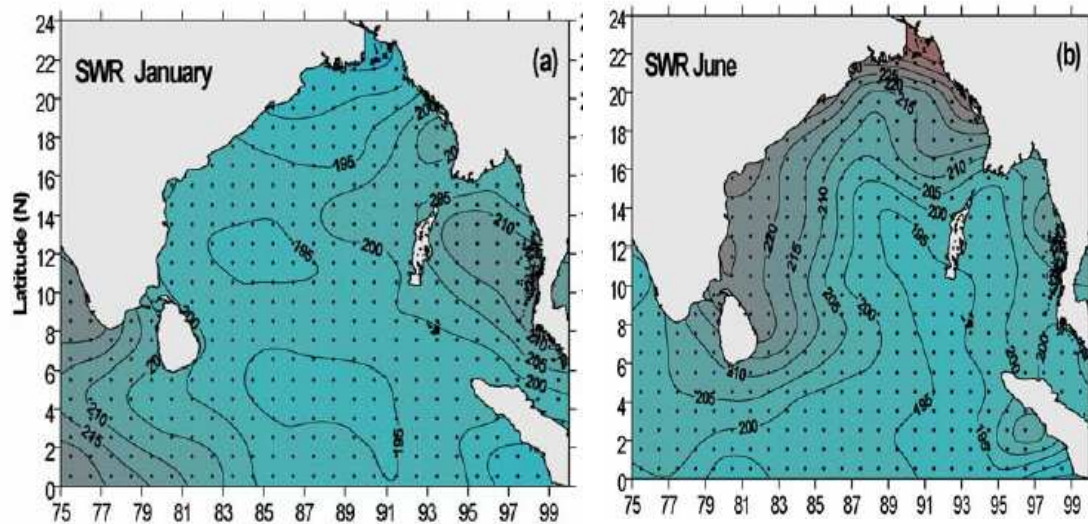


Fig.6.13 (A) Short wave radiation in Bay of Bengal January (a), June (b)

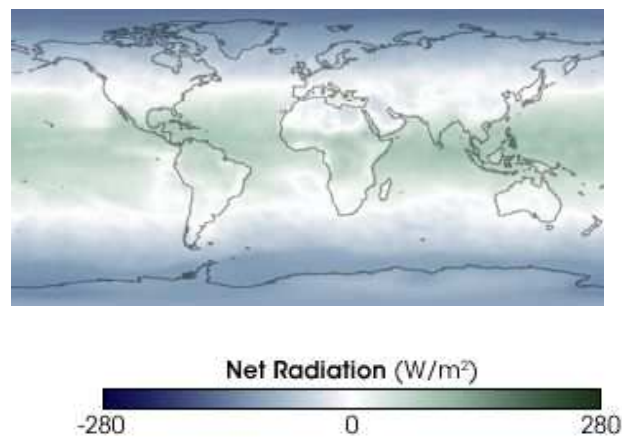


Fig.6.13.(B) Net radiation over the world during Sept 2005 (courtesy ERBE and CERES Projects, NASA LaRC)

A portion of the sunlight that reaches Earth is absorbed into the system, while some of the light is reflected by our planet back into space. Some of the sunlight that gets absorbed is converted to heat and later emitted by the surface and atmosphere back up into space. The term "net radiation" refers to the total amount of sunlight and heat energy that does not escape from the top of the Earth's atmosphere back into space. More precisely, net radiation is the sum total of shortwave and long wave electromagnetic energy, at wavelengths ranging from 0.3 to 100 micrometers, that remains in the Earth system. The image above (Fig.6.13B) is a false-color map showing the net incoming energy (in Watts per square meter) that was contained in the Earth system for the given month(s). Regions of positive net radiation indicate areas of energy surplus in the Earth system (i.e., green regions over the tropics) and areas of negative net radiation signify regions of energy deficit (such as blue regions over high latitudes and the poles). This image in

this dataset up to and including February 1990 was acquired by the Earth Radiation Budget Experiment (ERBE) sensor and by the Clouds and the Earth's Radiant Energy System (CERES) sensor aboard NASA's Terra satellite.

The value of Q_s depends on a number of factors, i) the length of the day, season and the geographic latitude and longitude, ii) absorption of short wave radiation by gas molecules, dust particles, water vapor etc. present in the atmosphere iii) elevation of the sun's position and iv) cloud amount. See figure 6.14 for the difference of Q_s in different months.

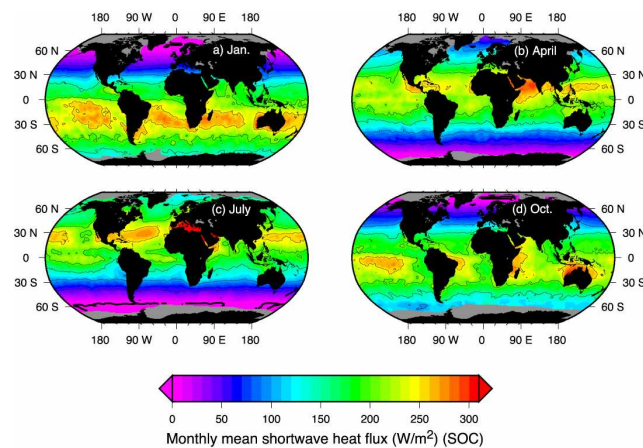


Fig.6.14. Monthly mean short wave heat flux Q_s (W/m^2) (By courtesy of www.nodc.noaa.gov)

6.2.3. EFFECT OF CLOUDS:

The effect of the cloud on insolation is given by the formula

$$Q_{sc} = Q_s (1 - 0.07 C)$$

where Q_{sc} is insolation reaching the earth's surface when 'C' amount of cloud is present, and Q_s is insolation with clear sky. For example if the sky is overcast, $C = 10$ then the insolation drop is 0.3 of Q_s which means 70% is lost.

Cloud fraction represents the portion of sky in each pixel that is covered by clouds. Satellites can measure cloud fraction over the entire atmosphere and for all types of clouds. Since most clouds reflect incoming sunlight very well and trap heat escaping from the Earth's surface, cloud fraction is an important parameter in studies of our planet's radiant energy budget. Fig.6.15 shows the cloud fraction during June 1991.

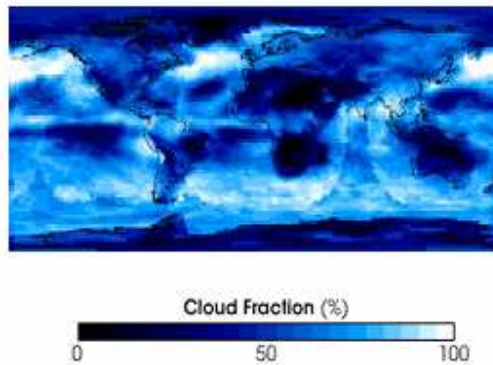


Fig.6.15 Cloud fraction during June 1991 (Data from International Satellite Cloud Climatology Project [ISCCP]).

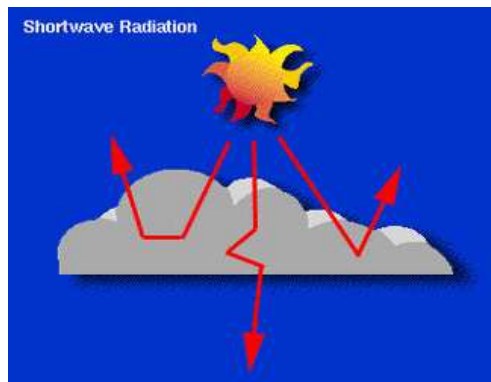


Fig.6.16. majority of short wave radiation reflects and scatters from thick cumulus clouds

Majority of the shortwave rays from the Sun are scattered and reflected into space by thick cumulus low clouds as shown by figure 6.16. The resulting "cloud albedo forcing," taken by itself, tends to cause a cooling of the Earth. Whereas Longwave rays emitted by the Earth are absorbed and reemitted by these clouds, with some rays going to the earth's surface back as shown by figure 6.17. Thicker yellow arrows indicate more energy. The resulting "cloud greenhouse forcing," taken by itself, tends to cause warming of the Earth.

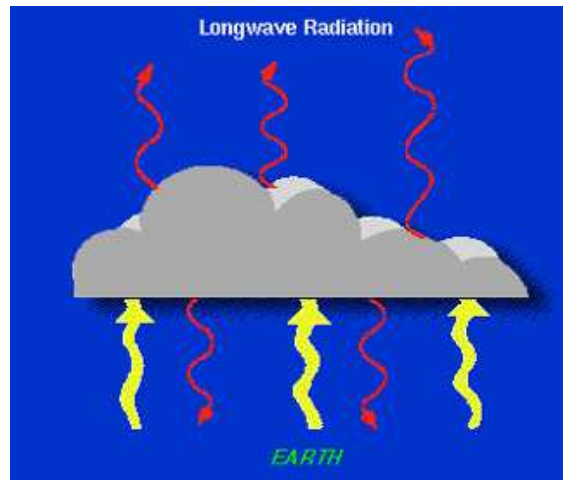


Fig.6.17. While cumulus clouds are transparent to the short wave radiation they are translucent to Long wave radiation from the earth (yellow) and so reradiates back.

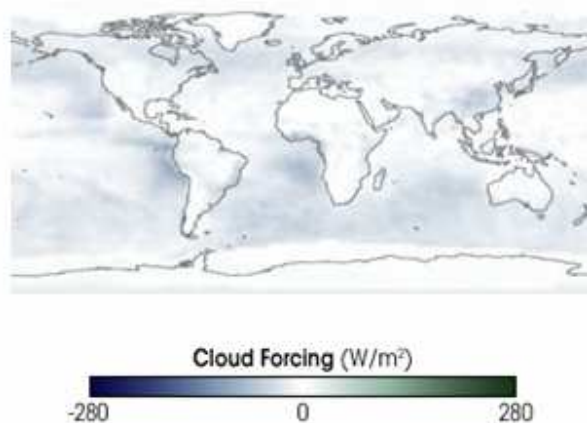


Fig.6.18. cloud forcing during September 2005 (Data courtesy ERBE and CERES Projects, NASA LaRC)

Clouds play a significant role in our world's energy balance. They exert both a cooling effect on the surface by reflecting sunlight back into space, and a warming effect by trapping heat emitted from the surface. Clouds are one of the greatest areas of scientific uncertainty with respect to how much they influence climate on a global scale. The term "cloud radiative forcing" refers to the effects clouds have on both sunlight and heat in the atmosphere. More precisely, cloud radiative forcing measures how much clouds modify the net radiation, at wavelengths ranging from 0.3 to 100 micrometers, of the Earth system. The image above (Fig.6.18) is a false-color map showing the magnitudes of cloud radiative forcing (in Watts per square meter) for the month of September 2005. Regions of positive cloud radiative forcing indicate areas where clouds act to increase net energy into the Earth system (i.e., regions of deep tropical convection) and areas of negative cloud radiative forcing signify regions where clouds act to decrease net energy into the Earth system (such as areas of stratus clouds).

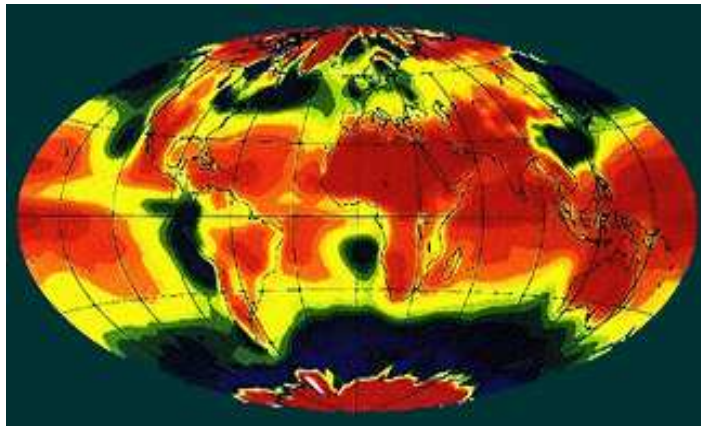


Fig.6.19. Annual average net cloud radiative forcing determined from 1985 to 1986. (Earth Radiation Budget Experiment data on the Earth Radiation Budget Satellite and the NOAA-9 satellite. Data processed at NASA Langley Research Center; images produced at the University of Washington).

Fig.6.19 is the net cloud forcing which is the result of two opposing effects: (1) greenhouse heating by clouds (or positive forcing) i.e. clouds trap heat coming from Earth's surface that would otherwise be lost to space, and (2) cooling by clouds (or negative forcing) i.e. clouds reflect incoming solar radiation back to space. The relatively large areas, where cooling is the greatest, are represented by colors that range from yellow to green and blue. In some areas, the effect of the clouds is to produce some warming as shown by colors that range from orange to red and pink. Overall, clouds have the effect of lessening the amount of heating that would otherwise be experienced at Earth's surface.

A final factor that effects insolation is the albedo (34%) as shown in Fig.6.18 and the sea state which is determined by Beaufort wind scale.

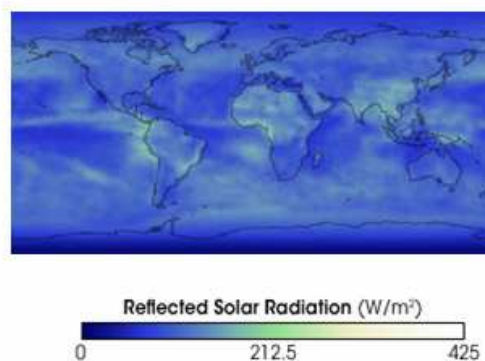


Fig.6. 20 .Albedo of the earth's surface (courtesy ERBE and CERES Projects, NASA LaRC)

A portion of the sunlight that enters the Earth system is reflected back into space by a combination of the clouds, aerosols, and gases in the atmosphere, as well as from the surface called albedo. The term albedo or “reflected shortwave radiation” refers to the sum total of all the shortwave electromagnetic energy, or sunlight at wavelengths ranging from 0.3 to 5 micrometers, that escapes from the top of the Earth's atmosphere back into space. The image (Fig.6.20) above is a false-color map showing the amount of shortwave energy (in Watts per square meter) that was reflected by the Earth system. In the image, the brighter, whiter regions show where more sunlight is reflected, while green regions show intermediate values, and blue regions are lower values. Notice that regions that are typically cloudy tend to reflect more shortwave energy, while the land surface reflects less than clouds, and the ocean reflects less than the land. This image was acquired by the Earth Radiation Budget Experiment (ERBE) sensor and by the Clouds and the Earth's Radiant Energy System (CERES) sensor aboard NASA's Terra satellite.

6.3. BACK RADIATION (Q_B):

A portion of the sunlight that enters the Earth system is reflected back into space, while the remaining portion of the sunlight is absorbed by the Earth system and stored as heat; some is absorbed in the atmosphere and some is absorbed in the land and oceans. A percentage of this stored heat is emitted by the Earth system back into space in the form of long wave energy. The term “outgoing long wave radiation” refers to the sum total of all the long wave electromagnetic energy, or infrared radiation at wavelengths ranging from 5 to 100 micrometers, that escapes from the top of the Earth's atmosphere back into space. The image (Fig.6.21) is a false-color map showing the amount of long wave energy (in Watts per square meter) that was emitted by the Earth system for the given month(s). In the image, the brighter yellow and orange regions show where more heat is emitted, while purple and blue regions show intermediate values, and white regions are lower values. Notice that most heat is escaping from the world's equatorial and desert regions. Notice also the tropical heat transported northeastward by the Gulf Stream in the Atlantic Ocean. This image was acquired by the Clouds and the Earth's Radiant Energy System (CERES) sensor aboard NASA's Terra satellite.

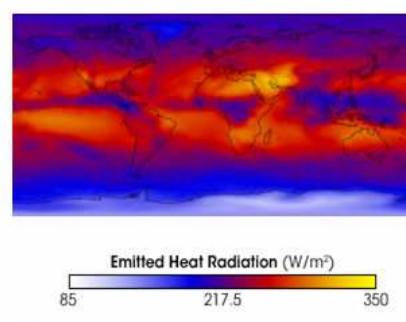


Fig.6. 21 Back Radaiaion Q_B over the earth during March 2000 (Data courtesy ERBE and CERES Projects, NASA LaRC)

The absorption of solar energy heats up our planet's surface and atmosphere and makes life on Earth possible. But the energy does not stay bound up in the Earth's environment forever. If it did, then the Earth would be as hot as the Sun. Instead, as the rocks, the air, and the sea warm, they emit thermal radiation (heat). This thermal radiation, which is largely in the form of long-wave infrared light, eventually finds its way out into space, leaving the Earth and allowing it

to cool. For the Earth to remain at a stable temperature, the amount of long wave radiation streaming from the Earth must be equal to the total amount of absorbed radiation from the Sun.

It is the effective long wave radiation given away from the ocean surface by virtue of emission of radiation as a black body that is governed by Stefan-Boltzman law. Back radiation depends on i) sea surface temperature ii) water vapor in the air and iii) cloud amount. The effect of cloud is given by the formula

$Q_{bc} = Q_b (1 - 0.08 c)$ where 'C' is the cloud amount. If the sky is overcast $C = 10$ and Q_{bc} will be 20% of Q_b , which means 80% is reduced.

Q_b also varies within the limits of 14% in tropical oceans. For example the variation of Q_b for the sea surface temperature (SST) of 10°C and 20°C can be computed with the help of Stefan-Boltzman law as

$$Q_b = \sigma T^4, \text{ therefore } Q_{b10} = \sigma (283)^4 = 225 \text{ ly/day taking } \sigma = 8.22 \times 10^{-11}$$

similarly $Q_{b20} = \sigma(293)^4 = 285 \text{ ly/day}$. Therefore, $Q_{b20}/Q_{b10} = 0.14$ (=14%).

Fig.6.22 shows the variation of Q_b in different months. In January large parts of Arabian Sea and Bay of Bengal lose high values of heat by back radiation (nearly 80 w/m^2), whereas in July it reduces to 40 w/m^2 . The reason for this is Indian region experiences clear sky conditions during January whereas in summer (July) atmosphere has frequent overcasting conditions so the back radiation is reduced due to re-radiation effect.

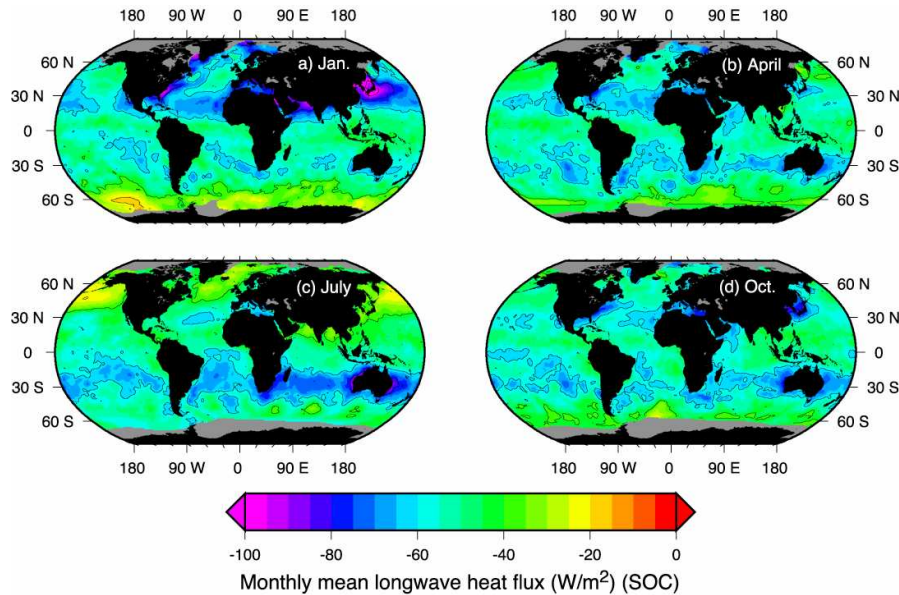


Fig.6. 22. Variation of Q_b in different months (By courtesy of www.nodc.noaa.gov)

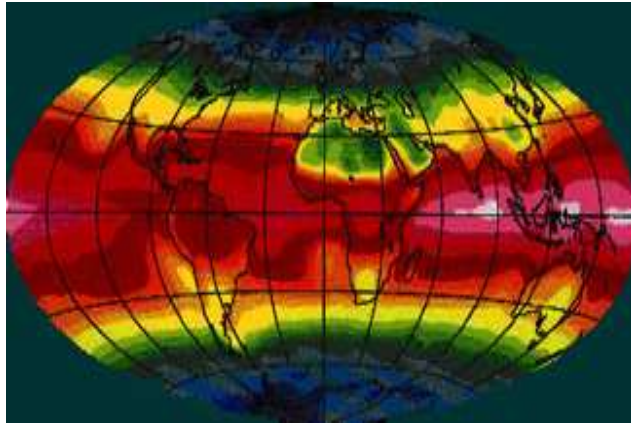


Fig.6.23 Annual average net radiation determined from 1985 to 1986

Fig.6.23 shows the net radiation which is the difference between incoming solar radiation that is absorbed by Earth and outgoing infrared radiation from Earth that is lost to space. The net radiation is generally positive at low latitudes (increases in heating represented by oranges, reds, and pinks) and negative at high latitudes (increases in cooling represented by greens and blues).

6.3.1. EFFECT OF WATER VAPOR ON Q_b :

With the increase of sea surface temperature the back radiation decreases. This is because a rise in SST causes an increase in the outward radiation from the sea but at the same time is accompanied by an increase in humidity as shown in fig.6.24. The warmer the air over the oceans, the more water it can hold before becoming saturated. Thus a given relative humidity value at a high temperature corresponds to a greater atmospheric water vapor content than the same relative humidity at a lower temperature. The more water vapor is in the atmosphere, the longer wave radiation is absorbed by it, and the more is radiated back to the sea, thus decreasing the net loss of long wave energy from the sea surface.

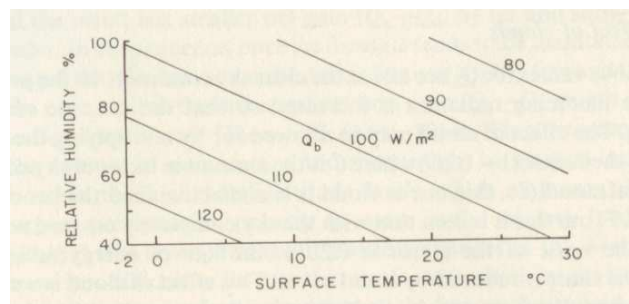


Fig.6. 24. Back radiation (Q_b) from the sea surface as a function of SST and R.H in the absence of cloud (Pickard, 1985)

6.4. SENSIBLE HEAT TRANSFER (Q_H):

When there is a temperature gradient, the heat will be conducted from high temperature region to low temperature region. If the temperature decreases upward from the sea heat is conducted from the sea to the atmosphere and in such case Q_h is a loss term to the sea and if temperature increases upward, conduction takes place from the atmosphere to the sea and Q_h is a gain term to the sea. The amount of loss or gain is given by the equation:

$$Q_H \text{ is proportional to } C_p \frac{dt}{dz} \text{ or } Q_H = -KC_p \frac{dt}{dz}$$

where 'K' is the coefficient of molecular thermal conductivity, C_p is the specific heat of air at constant pressure and dt/dz is the temperature gradient. The negative sign is assigned because the flow of heat will be towards the decreasing direction of temperature.

The coefficient of molecular thermal conductivity K, is a constant for a particular gas and for a particular temperature. However, in the applications of meteorological and oceanographical problems, particularly over the sea surface when the air is in motion it is turbulent. Hence the transfer of heat will be much more vigorous than the transfer of molecular motion. So in the case of turbulent motion the coefficient of molecular thermal conductivity is to be replaced by eddy conductivity of heat (A_h)

$$Q_H = -A_h C_p \frac{dt}{dz}$$

The value of A_h is not constant even at constant temperature. It depends on various factors such wind speed, size of the ripples waves, tides etc. in the oceans.

Fig.6.25 shows the sensible heat or conduction of heat loss from ocean to atmosphere in different months. In Arabian Sea and Bay of Bengal Q_h is negligibly small (close to zero) both in winter (January) as well as summer (July) because both the atmosphere and oceans are in same state.

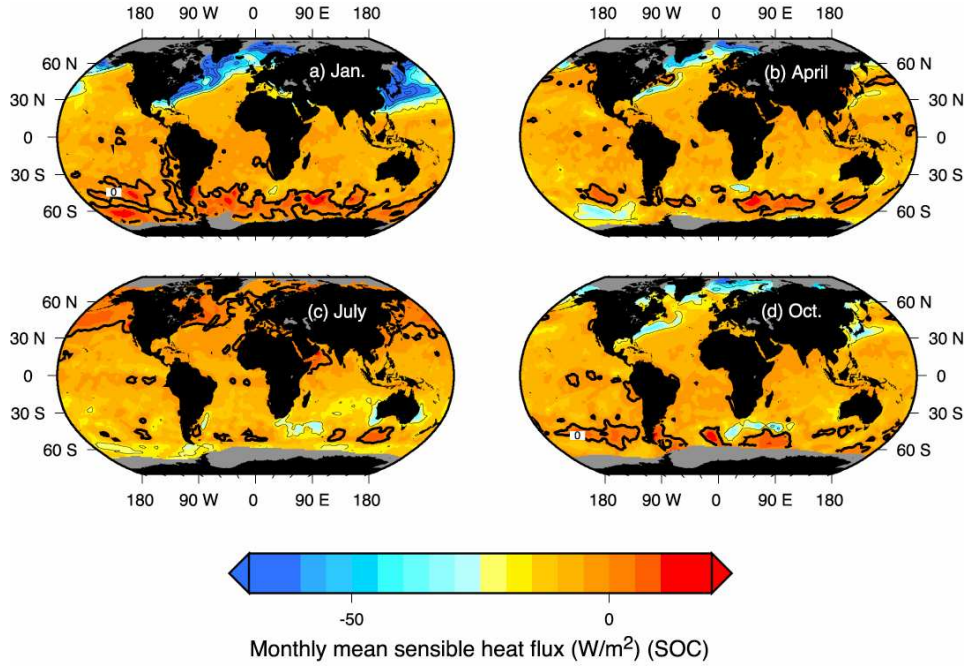


Fig. 6. 25. Variation of Q_h in different months. (By courtesy of www.nodc.noaa.gov)

6.5. EVAPORATION (Q_E) :

The evaporation term Q_E is included in the heat budget because for evaporation to occur it is necessary either to supply heat from outside or heat is to be taken from the remaining liquid.

$Q_E = (F_E \cdot L_T)$ where F_E is the rate of evaporation of water in grams per minute per square centimeter and L_T is the latent heat of evaporation in cal/gram. L_T is not constant and depends on temperature. For pure water L_T is given by:

$$L_T = 596 - 0.52 t \quad \text{where 't' is the temperature in } ^\circ\text{C}$$

$$F_E \text{ proportional to } \frac{df}{dz}, \quad F_E = -A_E \frac{df}{dz}$$

where $\frac{df}{dz}$ is the humidity gradient and A_E is eddy coefficient of diffusion which depends on wind speed, size of the ripples and waves.

$$\therefore Q_E = F_E \cdot L_T = -L_T \cdot A_E \frac{df}{dz}$$

The evaporation rates are lower (higher) over the Arabian Sea, during active (weak) monsoon conditions over the Indian subcontinent, indicating its insignificant role on the ensuing monsoon activity over the Indian subcontinent during the monsoon 2002 (Fig.6.26)

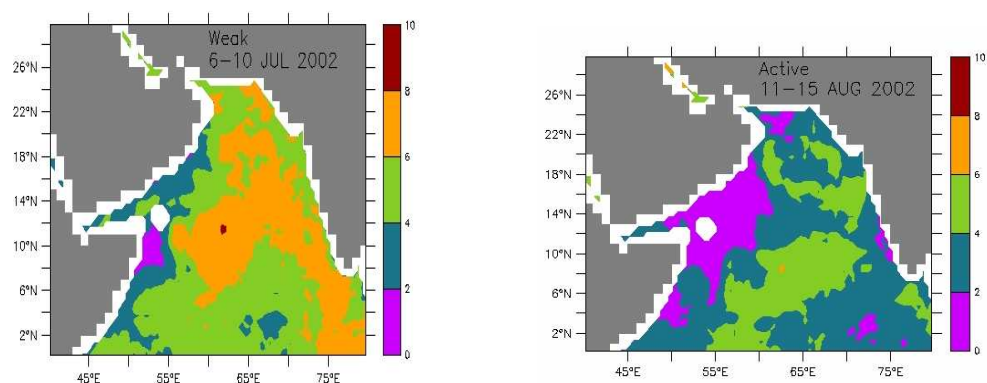


Figure 6.26. The evaporation rates over the Arabian Sea during two contrasting monsoon activity period over the Indian subcontinent a) Active monsoon conditions (11-15 August, 2002) and b) Weak monsoon conditions (6-10 July 2002). (Ramesh kumar et al 2002)

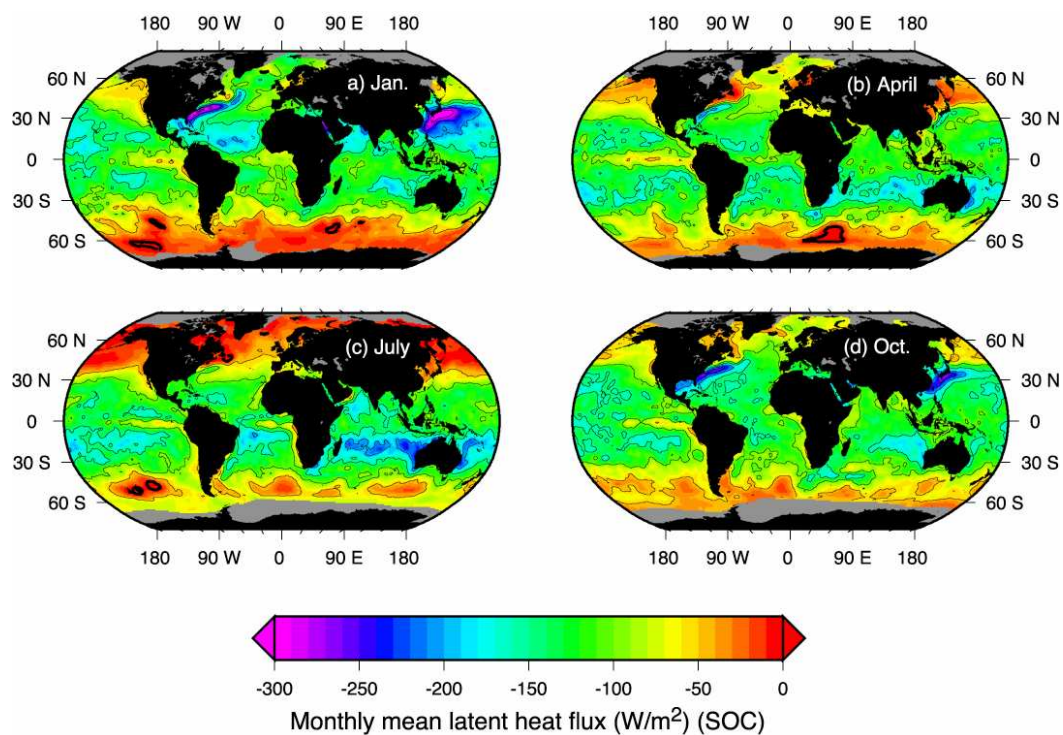


Fig.6.27 Variation of Q_E in different months. (By courtesy of www.nodc.noaa.gov)

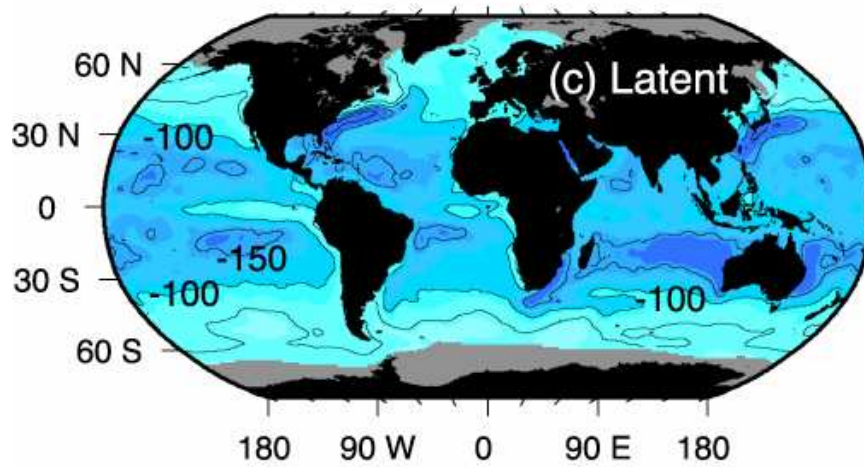


Fig.6.28 Global distribution of Q_E . (By courtesy of www.nodc.noaa.gov)

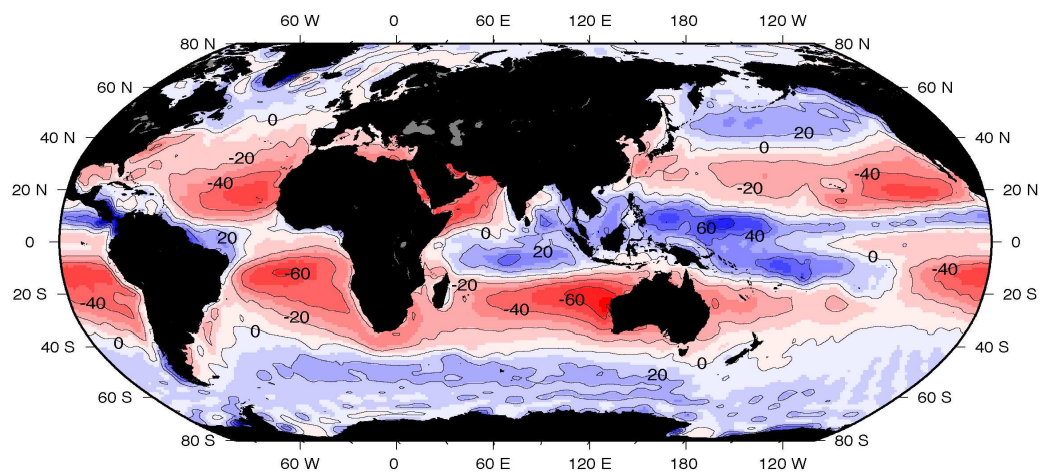


Fig.6.29 Global variation of Net evaporation – precipitation (red evaporation, blue precipitation) . (By courtesy of www.nodc.noaa.gov)

6.6. Distribution of heat budget components in the oceans:

Fig.6.28 and 6.29 show the variation of annual mean values Q_E and surplus or deficit energy resulted from evaporation minus precipitation respectively. The monthly variation of Q_H and Q_E are shown in Figs.6.25 and 6.27. While in north Indian Ocean most of the time the latent heat flux is between 100 to 150 W m^{-2} , the flux goes to about 200 W m^{-2} during January and July. Both the terms critically depend on the degree of turbulent convection taking place in the atmosphere above the sea surface. So Q_H and Q_E depend on vertical temperature and humidity gradients respectively.

As in most of the areas of the ocean, the sea surface in the Pacific Ocean (Fig.6.30) is warmer than the overlying air, so heat is lost from the sea and so is minus (-ve) on the other hand if the sea surface is cooler than the overlying air the heat is gain to the sea and so positive(+ve). One of the few regions of the ocean where Q_E is positive is the Grand Banks of New Found land in North Atlantic. Here fogs are very common due to condensation occurring as a result of warm, moist air coming into contact with a cold sea surface. This type of fog is known as advection fog. The reason for the high negative values of Q_h in the western ocean off Japan and eastern shores of U.S.A is due to the presence of Kuroshio Current & Gulf Stream which are warm currents. The water carried from low latitudes by Kuroshio & Gulf Stream is significantly warmer than the overlying air and so the transfer of heat from sea to air by conduction is above average here (Fig.4.12 Jan). In addition, warming air from below at the point of contact of sea surface encourages turbulent convection and so leads to negative values of Q_h . Similarly the positive values of Q_h off Peru coast are due to the presence of cold Peru Current (El Nino). In eastern equatorial Pacific, SSTs are very low because of high amount of upwelling. As the air above is warmer (due to equatorial climates) while the sea surface is colder naturally conduction takes place towards the sea. So Q_h is positive.

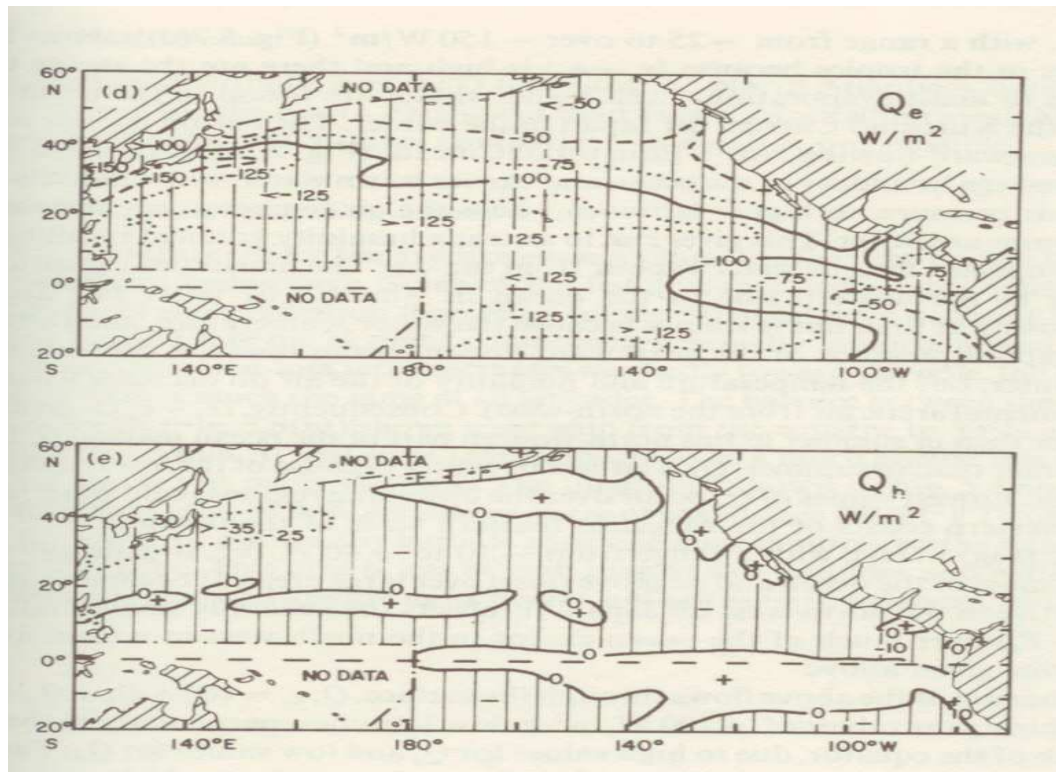


Fig.6. 30. Variation in annual mean values of Q_E , and Q_h in the North Pacific. +ve values = gain, -ve values = loss to the sea.(Pickard,1985)

Monthly variation of surface heat flux in the Baltic Sea is shown in Fig.6.30 a. Where Q_{in} is net heat flux, Q_s is incoming solar radiation, Q_c is sensible heat flux, Q_E is heat flux due to evaporation and Q_b is back radiation. One may note the sensible heat flux is positive during April to July in Baltic Sea. This means sea gains heat from the atmosphere in this period.

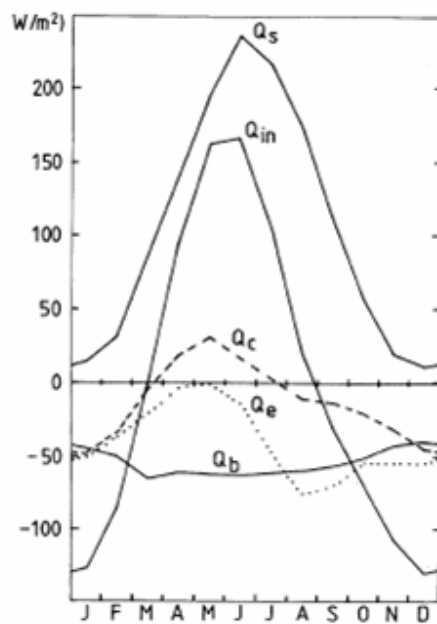


Fig.6.30a Monthly variation of heat budget parameters in the Baltic Sea (By courtesy of Rohde,J,1998)

6.7. BOWEN'S RATIO:

Because of the uncertainty in the values of A_h and A_E , it is not possible to compute Q_H and Q_E directly. Bowen introduced a method by which Q_H and Q_E can be evaluated from the heat budget equation: $Q_S = Q_b + Q_h + Q_E$

In this Q_S and Q_B can be measured using the pyranometer and radiometer.

$$Q_S - Q_B = Q_H + Q_E$$

$$(Q_S - Q_B)/Q_E = \left[\frac{Q_H + Q_E}{Q_E} \right] = 1 + \frac{Q_H}{Q_E} = 1 + R$$

$$\therefore Q_E = \left(\frac{Q_S - Q_B}{1 + R} \right)$$

$$\text{or } Q_H = \left(\frac{Q_S - Q_B}{1 + \frac{1}{R}} \right) \dots\dots\dots (4.1)$$

This R is called Bowen's ratio. If we can determine R, either Q_H or Q_E can be determined in an indirect way. As quantifying Q_H and Q_E is difficult, they can be estimated if we can estimate R

and R can be estimated using the vertical gradients of heat ($\frac{dt}{dz}$) and water vapor ($\frac{df}{dz}$) as given below. Also as long as radiation terms (Q_H , Q_E) or net radiation term ($Q_S - Q_B$) is available we can estimate R.

$$\frac{Q_H}{Q_E} = \frac{-A_H C_P \frac{dt}{dz}}{-L_T A_E \frac{df}{dz}}$$

Substituting the values of Q_H and Q_E in $R =$

A_H and A_E being the coefficient of eddy thermal conductivity and coefficient of eddy diffusivity. Hence under similar conditions the numerical value of these two terms can be assumed to be same values. So $A_H = A_E$

$$R = \frac{C_P \frac{dT}{dz}}{L_t \frac{df}{dz}} \quad \text{if } \frac{df}{dz} \text{ is written in terms of vapor pressure units using the formula}$$

$\frac{df}{dz} = \frac{0.621}{p} \frac{de}{dz}$ where p is the atmospheric pressure expressed in millibar and $\frac{de}{dz}$ is the vapor pressure gradient.

$$\therefore R = \frac{p}{0.621} \frac{C_P}{L_t} \frac{dt/dz}{de/dz} \quad \text{if we assign suitable temperatures and vapor pressures within a}$$

$$\frac{dT}{dz} = \frac{T_S - T_a}{Z_1 - Z_2}, \quad \frac{de}{dz} = \frac{e_s - e_a}{z_1 - z_2}$$

sufficient layer of thickness between the heights Z_1 and Z_2

$$\therefore R = \frac{p}{0.621} \frac{C_P}{L_t} \frac{T_S - T_a}{e_s - e_a} \quad \text{Substituting standard values of } p=1000 \text{ mb, } C_p=0.24 \text{ and } L_t = 580 \text{ cal,}$$

$$R = 0.66 \frac{T_S - T_a}{e_s - e_a}$$

By measuring the temperatures and aqueous vapor tension at the sea surface and anemometer level (ten meters) above the sea surface R can be calculated. Thus Bowen's Ratio is defined as the ratio of sensible heat to latent heat loss.

The average value of R in the tropical oceans is about 0.1 which implies that the latent heat loss in the oceans is ten times greater than the sensible heat loss. This value increases to about 0.45 at 70°N latitude. Which means R increases with increase of latitude implies Q_H proportion increases from Q_E in the Bowen's Ratio. Lower the values of R, the higher will be the

evaporation. Usually R will be positive because the average sea surface temperature is higher than the average air temperature by about 0.8°C .

A negative value of R indicates gain of heat by the oceans which can occur when the sea surface temperature is lower than the air temperature or when condensation takes place on the sea surface.

The value of R will be the lowest in the subtropical regions in winter particularly on the western sides of the oceans where maximum evaporation takes place. Towards the equator the value of R increases slightly. The higher values of R occur during summer in high latitudes which imply that sensible heat loss is much more there compared to low latitudes.

The Fig 6.31 represents the variation of mean annual values of heat budget equation in the N.H. This implies for the oceans as a whole, the heat gained is equal to the heat lost at least for a long period. Then we can consider $Q_T = 0$. But the question is when there is a net gain of heat in the equator ward from 38°N and a net loss poleward how can for a given location Q_T is zero. This can be explained only by means of general circulation of the oceans. That is the advective term (Q_V) in the heat budget term is to be considered important. Warm currents flow towards high latitudes and cold currents flow towards low latitudes for transport of heat or cold. Thus over a period of year the mean temperature of the oceans remains constant.

Another important point to be borne in mind with respect to Fig.6.31 is the hatching area above and below the curve from the mean indicates the heat gain and loss below and above 38°N respectively. You may note that the area of gain appears to be less than that of the loss and there is no balance. Although in the figure it appears different but both the areas are equal as due to sphericity of the earth at high latitudes it appears to be truncated. This implies that the radiation balance changes from a net surplus to a net loss at about 38° latitude (Subtropical highs) in each hemisphere.

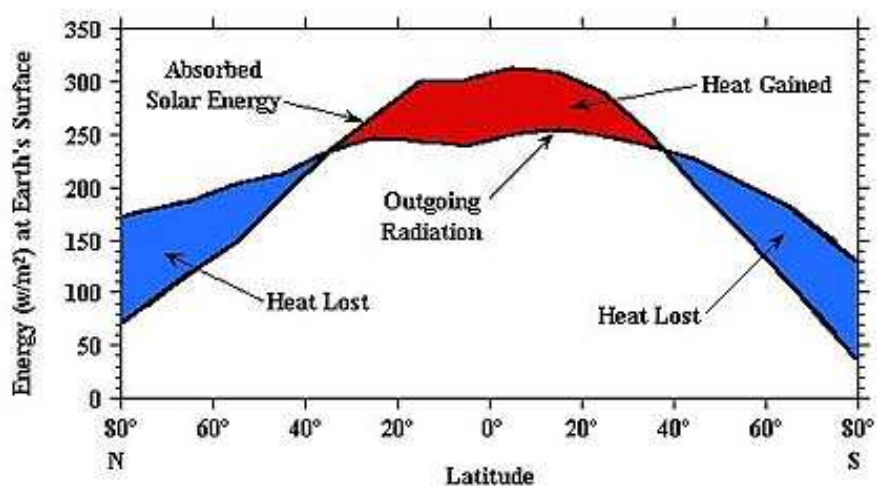


Fig. 6.31 variation of heat gain minus heat loss with latitude (www.physicalgeography.net)

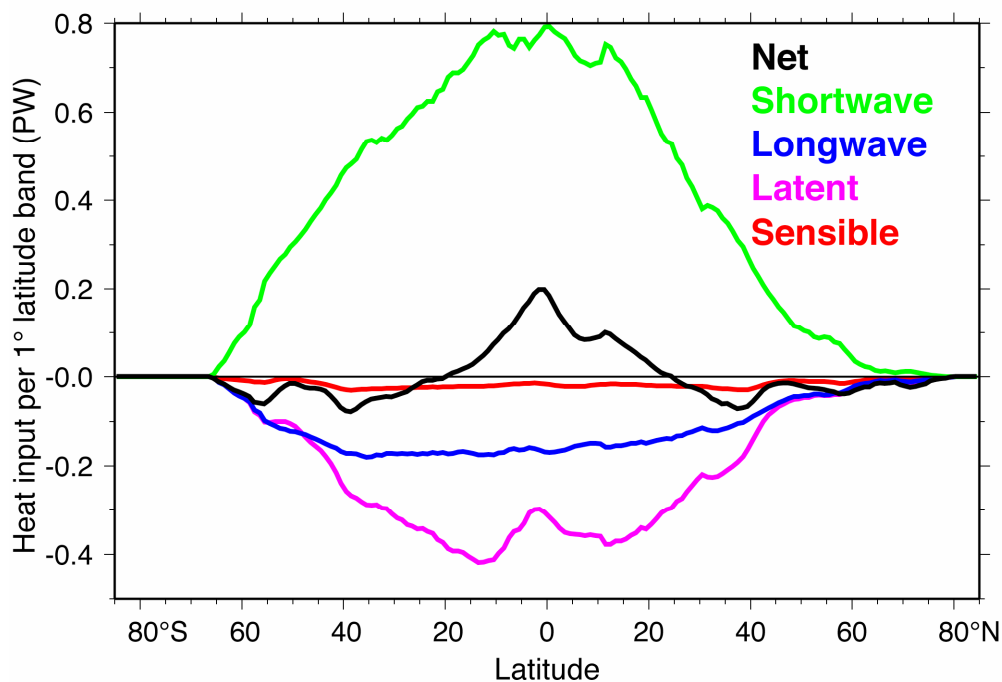


Fig.6.32 Heat flux components summed for latitude bands (Peta Watts/m²). Zonal averages of heat transfer to the ocean by Q_s (short wave), Q_l (long wave), Q_h (Sensible), Q_e (latent heat) and net heat flux calculated by DaSilva, Young and Levitus (1995) (By courtesy of www.nodc.noaa.gov)

Fig.6.32 shows the values of different terms of the heat budget in the zonal average. The zonal average is an average along the lines of constant latitude. The zonal average of the oceanic heat budget terms shows that insolation (green curve) is greatest in the tropics, evaporation (pink curve) balances the insolation and the sensible heat flux (red) is small. Note that the net heat flux (black curve) in the figure (6.32) do not sum up to zero, because the net heat flux into the ocean averaged over several years must be less than a few watts per square meter and the non-zero value must be due to errors in the various terms in the heat budget. Thus the resulting meridional heat transport across the latitudes is shown in Fig.6.33.

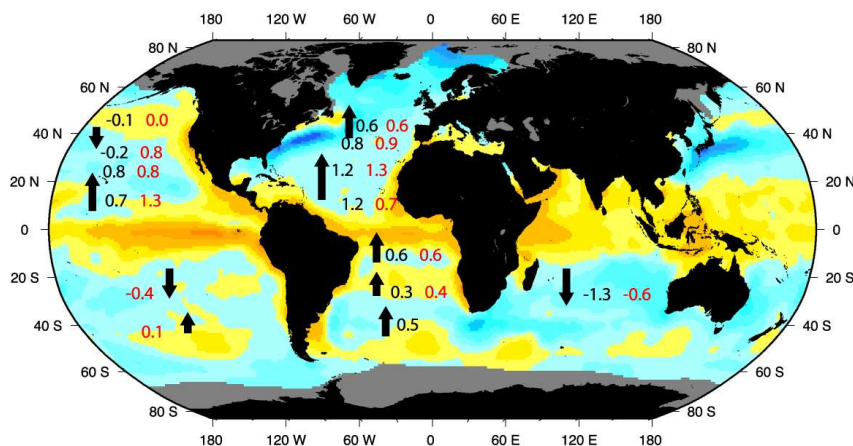


Fig. 6.33 Meridional heat transport across each latitude in PW (Peta watts) (By courtesy of www.nodc.noaa.gov)

6.8. Heat Budget of the Indian Ocean:

In the Indian Ocean, the mean heat flux per unit area north of 20°S is about 40 W m⁻². Hastenrath and Lamb (1980) estimated that this heat energy has to be exported southwards across the Indian Ocean equator at an annual rate of about 0.5×10^{15} watts. This is equivalent to the average upwelling velocity of 6×10^{-5} cm s⁻¹ from 2000m over the whole Arabian Sea and the Bay of Bengal. This rate of upwelling velocity is large compared to that of the global upwelling rate 4×10^{-5} cm s⁻¹.

One might easily guess that the reason for such a relatively large heat flux and large deep upwelling velocity is due to the confinement of the Tropical Indian Ocean (TIO) in the low latitudes. The insolation is the strongest in the tropics and so the heat flux is high in the TIO. This large heat flux is distributed by two agencies viz., the meridional overturning cells and the horizontal wind driven gyres in the upper ocean. In the latter case, the subtropical gyres carry heated water from the tropics into midlatitudes and lose heat and so a negative zonally averaged surface heat flux results in the mid latitudes. The equatorial gyres, on the other hand, confine the heated water in the tropics and thereby reinforcing the heat input in the tropics leaving very little for meridional overturning for distribution of heat. That is why tropics act as heat sources. It is estimated that the south Indian Ocean exports heat to the higher latitudes at a rate of 0.69×10^{15} watts at 32°S.

Latent heat flux represents the heat lost through evaporation at the sea surface. The evaporation is highest in the subtropics and slightly less in the tropics. It varies from east to west across the ocean also. It is high (< -140 W/m²) in the Arabian Sea during December - January; in the central Arabian Sea during June-July; in the northern Bay of Bengal during December, April and June; along the southern boundary of Bay of Bengal during June; in the southern subtropical Indian Ocean (10° S to 25° S) during May-August and in the south-eastern Indian Ocean during April and September –January.

It was reported in 1989 high latent heat flux over the northwestern Arabian Sea and the Bay of Bengal and low latent heat flux over the southeastern Arabian Sea (because of weak winds) during the northeast monsoon; and high latent flux in the southeastern Arabian Sea (including the Lakshadweep Sea) in April.

Sensible heat flux represents the heat leaving the sea surface by conduction. It mostly varies between 0 and -15 W/m² indicating that, in general, SST is more than air temperature in the TIO, except in the region off Somalia and Arabia (associated with low SSTs) during summer monsoon (June to September). It is less than -10 W/m² in the northern Arabian Sea during December – January; in the eastern Bay of Bengal during June; in the southern sub-tropical Indian Ocean (south of 10° S) during May-September; and in the south-eastern Indian Ocean during October-December and April.

Net surface heat flux represents the net heat gain or loss at the ocean surface. It varies between $+160$ and -160 W/m^2 in the TIO. It is more than 100 W/m^2 in the northwestern and western Indian Ocean (north of 10° S) and in the Bay of Bengal during March-April; in the Arabian Sea and northern Bay of Bengal during July -August; off the Somalia and Arabia coasts and in the western Indian Ocean during September-October. It is less than -40 W/m^2 in the northern Arabian Sea during December-January; in the northern Bay of Bengal during December and in the southern subtropical Indian Ocean (south of 10° S) during May-August.

It was also found in the southern tropical Indian Ocean, gain of heat during austral summer and loss of heat during austral winter. In the Arabian Sea, north of 10° S , loss of heat during peak of both the monsoons and gain of heat during the transition periods between the monsoons and in the Bay of Bengal and over most of the equatorial Indian Ocean, gain of heat throughout the majority of the year.

During boreal winter, under the influence of dry and cold northeasterly winds, the net surface heat flux cools the north Indian Ocean, northwestern Arabian Sea and northwestern Bay of Bengal. During the pre-summer monsoon season, due to clear sky conditions, the net surface heat flux warms the surface in the region north of 20° S , with increasing amplitude toward the north. Maximum heating occurs over the northern Arabian Sea and northern Bay of Bengal. During the summer monsoon season, the net surface heat flux produces a dramatic cooling over the entire TIO with an exception of a band off Arabia where SST is cooler because of coastal upwelling. The cooling is also pronounced over the southwestern TIO, central Arabian Sea and eastern Bay of Bengal. During the post-summer monsoon season, the net surface heat flux warms the entire Arabian Sea, with maxima in the southwestern region where insolation is high and evaporation is low because of the presence of cold upwelled waters at the surface. The net surface heat flux also causes a mild warming in the region south of 20° S and a mild cooling in the rest of the TIO.

Figure 6.34 presents the moisture flux divergence/convergence at the sea surface over the tropical Indian Ocean. The most interesting feature of this figure is the region of large scale convergence (dashed area) in the eastern Indian Ocean, especially Bay of Bengal area. This indicates that this region is highly conducive for large scale convective activity like the formation of monsoon depressions and tropical cyclones round the year. From this it can be seen that the evaporation exceeds precipitation over all the tropical Indian Ocean except the eastern half of it. Thus it further emphasizes the role of the Arabian Sea and the cross equatorial moisture flux than the moisture from the Bay of Bengal region for the summer monsoon rainfall over the Indian subcontinent.

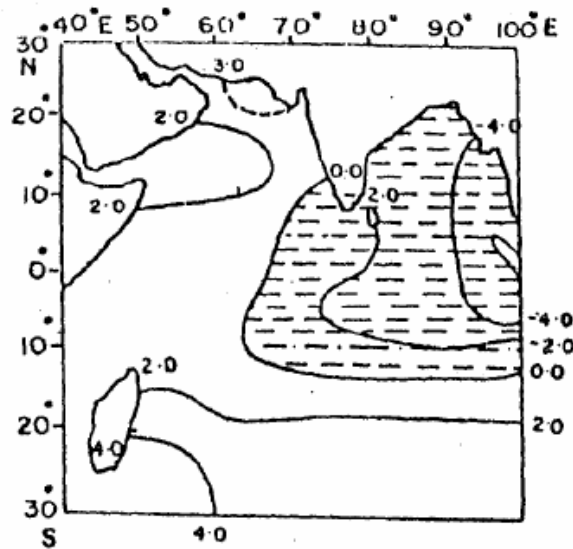


Fig.6. 34 Mean annual net flux divergence over the Tropical Indian Ocean (Nayak R.K, 2005)

6.8.1. Arabian Sea Cooling:

a) Summer cooling:

Arabian Sea is probably the only region in the world ocean which cools during summer. The cooling of the Arabian Sea is mainly caused by the surface heat exchange processes and lateral and vertical advection. During the Indo-Soviet Monsoon Experiment (ISMEX-73), it was observed significant fall (of about 1°C) in the temperature of the surface waters in the eastern Arabian Sea (along 71.5°E) from May to July. In a review of summer cooling of the Arabian Sea, it has been concluded that the entrainment of cold waters into the surface layer and the subsequent turbulent mixing play a dominant role in decreasing SST in the east central Arabian Sea. In the western Arabian Sea, upwelling and spreading of cold upwelled waters off Somalia and Arabia are the major processes for lowering of the SST. Thus it is clear that coastal upwelling plays a major role in the summer cooling of the Arabian Sea. A study of SST variability between May and August revealed that the regions of maximum cooling are the coastal regions off Somalia ($>5^{\circ}\text{C}$), Arabia ($>4^{\circ}\text{C}$) and southwest coast of India ($>3^{\circ}\text{C}$).

b) Winter cooling:

The northern Arabian Sea (especially north of 10°N) experiences a net heat loss from October to December. The cool dry continental air brought into the northern Arabian Sea by the prevailing northeast trade winds enhances evaporation. A combination of enhanced evaporation and the reduction in the solar radiation (from October to January) results in significant decrease of SST and presence of cold surface waters (25°C) in the northern Arabian Sea during winter (January-February). SST cooling in the Gulf of Oman during winter monsoon 1993 was also recorded. Cold SST evolves in the Gulf during an intense outbreak of winter winds. The turbulence generated by these winds in the surface atmospheric boundary layer depletes large heat from the sea surface and causes $1-2^{\circ}\text{C}$ SST cooling during January-March. The alongshore component of the wind stress promotes Ekman dynamics and further enhances SST cooling along

the periphery of the Gulf. A study of 4 year mean SST pattern off the west coast of India using AVHRR data showed a strong cooling north of 15° N and cold surface waters (25° C) along the Gujarat Shelf due to surface heat depletion during winter monsoon (December- March).

6.8.2. Evaporation in the Bay of Bengal:

In the Indian Ocean mean annual evaporation shows two maxima. One is (>170 cm) between 10°-20°S and 70°-90°E, and the other is (>130 cm) off the Somali coast between 0°-10°N and 45°-65°E. These two maxima are observed throughout the year except during September-November when the northwestern maximum subsides to a minimum (< 20 cm per quarter). Throughout the Bay while yearly mean values are 100-110 cm yr⁻¹ winter and summer mean values remain almost same about 30 and 30-35 cm/quarter respectively. This means yearly and seasonal means are also same. Comparatively the Arabian Sea experiences more evaporation in all seasons except in the post-monsoon period of September-November. Table 4.1 presents the seasonal evaporation rates for winter and summer means (shown in red italics) for different zones in the Bay of Bengal.

Latitude belt (°N)	Longitudinal belt (°E)				
	80-85	85-90	90-95	95-100	Mean
>20	-	34.25	28.44	-	31.34
	-	<i>26.78</i>	<i>30.46</i>	-	<i>28.62</i>
15-20	36.51	31.58	26.48	22.57	31.52
	<i>34.89</i>	<i>30.45</i>	<i>34.09</i>	<i>27.39</i>	<i>31.71</i>
10-15	37.32	35.61	29.27	33.15	33.84
	<i>36.77</i>	<i>40.16</i>	<i>33.33</i>	<i>30.10</i>	<i>35.09</i>
5-10	38.86	39.41	37.60	39.87	38.94
	<i>39.95</i>	<i>41.21</i>	<i>43.88</i>	<i>34.83</i>	<i>39.94</i>
Mean	37.56	35.21	30.45	31.86	-
	<i>37.20</i>	<i>34.63</i>	<i>35.44</i>	<i>30.77</i>	-
Grand mean					33.77
					<i>34.51</i>

Table: 4.1 Evaporation (cm/season) over Bay of Bengal in winter and summer (*red-italics*).

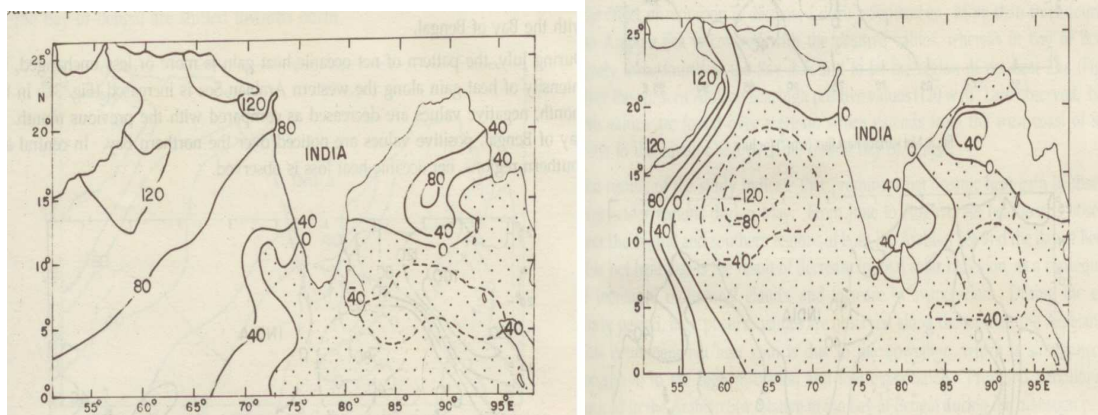


Fig. 6. 35 Net surface heat flux of the north Indian Ocean during May(left) & June(right). (By courtesy of V.Simhadri Naidu et al (1992): Physical Processes in the Indian seas,(ISPSO,1990) 11-16pp)

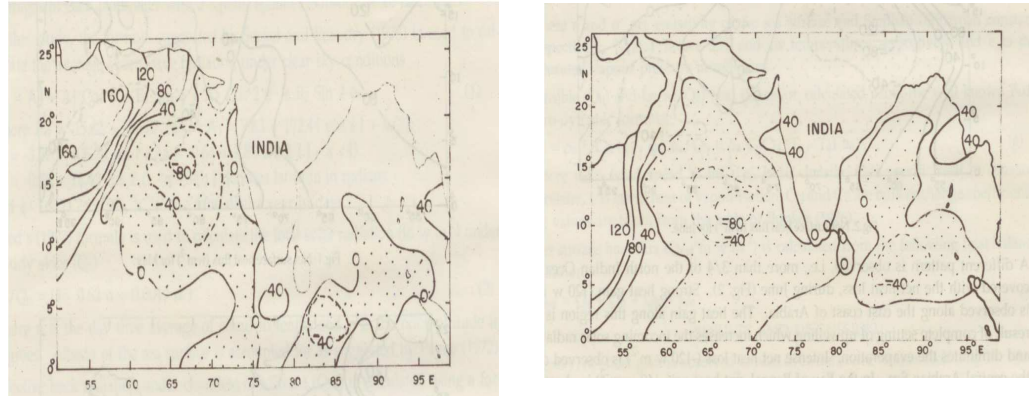


Fig. 6. 36 Net surface heat flux of the north Indian Ocean during July (left) & August (right). (By courtesy of V.Simhadri Naidu et al (1992): Physical Processes in the Indian seas,(ISPSO,1990) 11-16pp)

The methodology of Stevenson (1982) is adopted to compute the net surface heat fluxes at sea surface after reducing the meteorological data collected at different heights to a standard anemometer level (10m). According to him the net surface heat flux Q_N (W m^{-2}) is given by:

$$Q_N = Q_1 (1-\alpha) - Q_B - Q_E - Q_S$$

where Q_1 is the short wave radiation incident at sea surface, α is the albedo, Q_B is the effective back radiation and Q_E & Q_S are the latent and sensible heat fluxes.

Net surface heat flux of the north Indian Ocean during south west monsoon is shown in the Figure 6.35 & 6.36. In May (left figure 6.35) the net heat gain is observed almost over the entire Arabian Sea. Maximum positive values of 120 W m^{-2} are observed off the east coast of Arabia. Starting from Northwest in Arabian Sea to south east in Bay of Bengal the distribution changed from high heat gain of 120 W m^{-2} to a heat deficit of -40 W m^{-2} (Fig.6.35). In June this heat deficit area increased and spread towards Arabian Sea and a maximum deficit of -120 W m^{-2} occurred in central Arabian Sea (right figure of 6.35). The same situation, by and large, prevails during July & August also (Fig. 6.36). Here one interesting aspect to be noted is that throughout the southwest monsoon period (here in all the four months) the high surface heat gain of 120 W m^{-2} continued to exist all along the coast of Arabia and Horn of Africa. The reason for this high gain of heat flux is due to upwelling all along these coasts. Due to low SST values during upwelling naturally gain of heat from the atmosphere is expected.

6.8.3. Monthly Net heat balance

During January, net heat flux is negative in the northern Indian Ocean and is positive in the southern Indian Ocean (Fig.6.37). The maximum heat loss of 75 W m^{-2} is observed in the

central Arabian Sea. January being southern summer, more insolation is received over the southern Indian Ocean. The maximum values are observed in the regions south of 15°S . During the month of April, the net heat flux is positive over the Arabian Sea and Bay of Bengal where as it is negative in the southern tropical Indian Ocean. Maximum insolation is received in the Bay of Bengal and Arabian Sea during April. During July, the net heat flux is negative throughout the tropical Indian Ocean including Bay of Bengal and Arabian Sea. This is due to heavy evaporation in the summer season. By October, the heat flux is again positive throughout the tropical Indian Ocean due to excess insolation. As the wind is weak during the transition month of October, there is less evaporative heat loss and hence the net heat flux is positive.

6.8.4. Fresh water flux

During January, the (P-E) term is positive in the equatorial regions (Fig.6.38). January is the time when the ITCZ is just south of the equator. This gives more precipitation in the equatorial band and hence (P-E) term is positive. In the north Indian Ocean north of 10°N , evaporation is excess over precipitation and hence the (P-E) term is negative in January. In April, equatorial regions are characterized by positive (P-E) indicating excess precipitation over evaporation. During July, the regions north of 10°S are under the influence of southwest monsoon winds and there is heavy rainfall. Hence (P-E) term is positive in the equatorial belt; however, (P-E) term is negative in the western Arabian Sea (-2 mm/day) because of excess evaporation over precipitation during the monsoon months. Over the subtropical high pressure zone, (P-E) is negative due to excess evaporation.

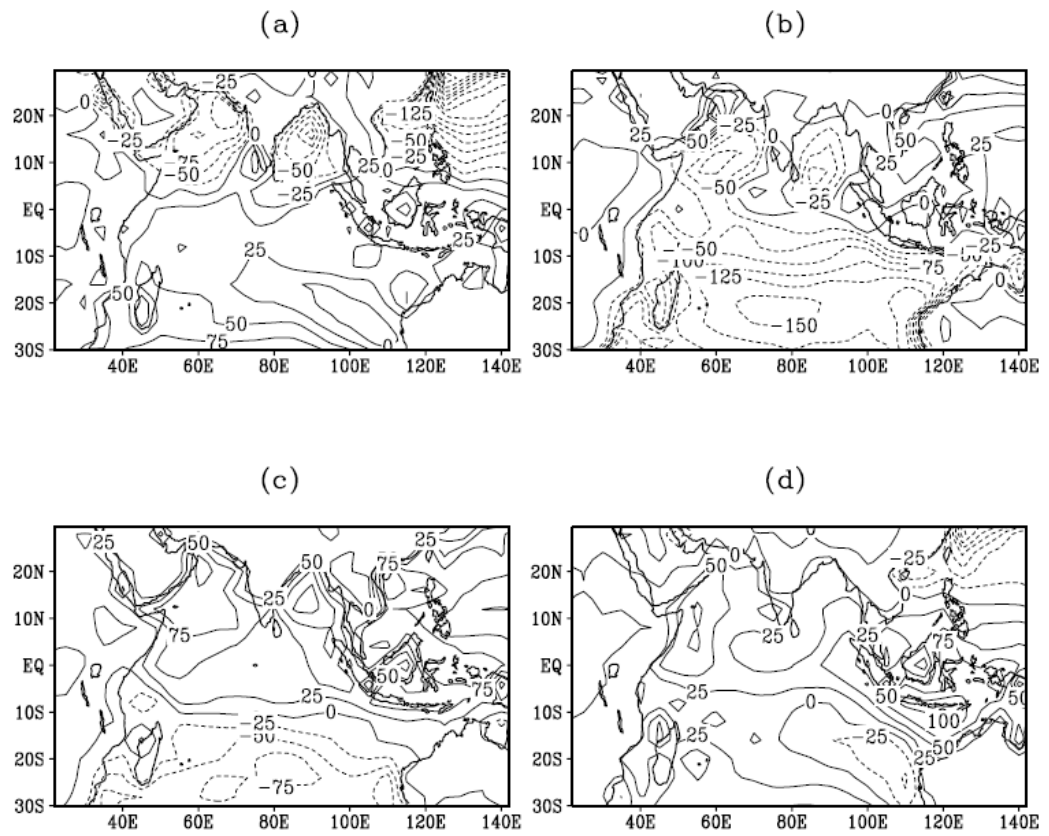


Fig.6.37 Spatial distribution of net heat flux (W m^{-2}) for (a)January, (b) July, (c) April and (d) October

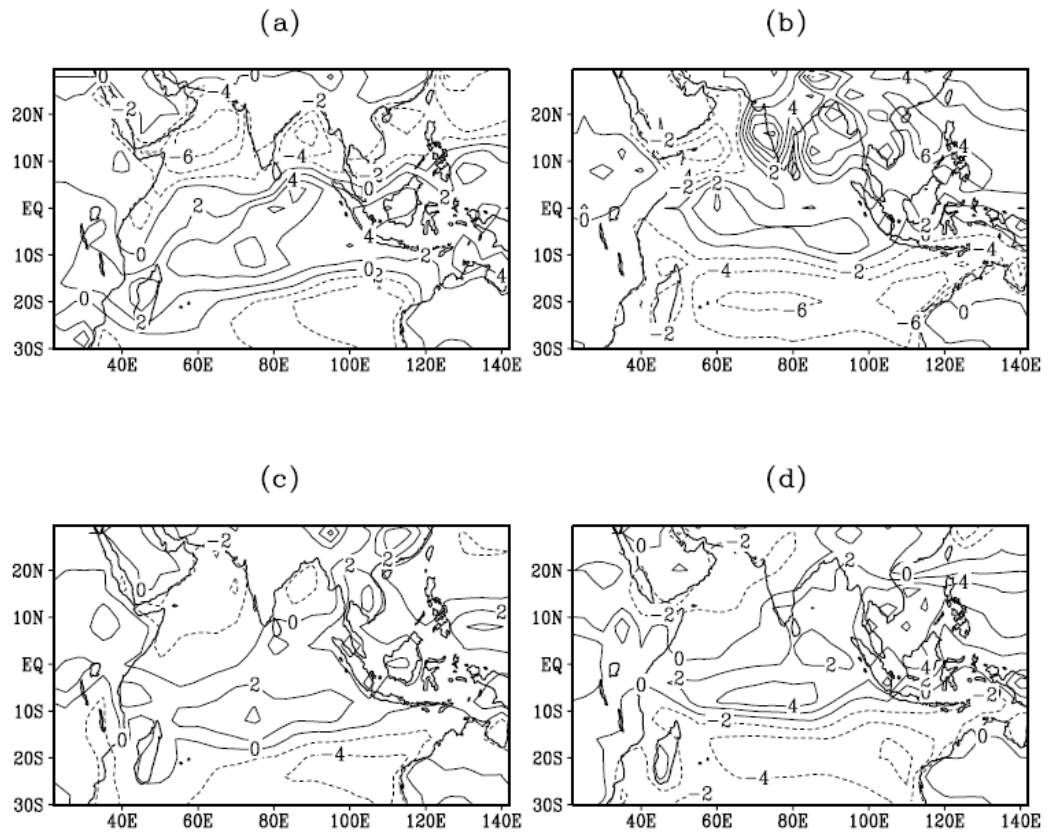


Fig.6. 38 Difference between precipitation and evaporation (P-E) in (mm/ day) for (a)January, (b) July, (c) April and (d) October

